Article

IDPConformerGenerator: A Flexible Software Suite for Sampling the Conformational Space of Disordered Protein States

Published as part of The Journal of Physical Chemistry virtual special issue "Protein Folding and Dynamics—An Overview on the Occasion of Harold Scheraga's 100th Birthday".

João M. C. Teixeira,* Zi Hao Liu, Ashley Namini, Jie Li, Robert M. Vernon, Mickaël Krzeminski, Alaa A. Shamandy, Oufan Zhang, Mojtaba Haghighatlari, Lei Yu, Teresa Head-Gordon, and Julie D. Forman-Kay*

Read Online

ACCESS | 📊 Metrics & More | 📄 Article Recommendations | 🔷 Supporting Information

ABSTRACT: The power of structural information for informing biological mechanisms is clear for stable folded macromolecules, but similar structure–function insight is more difficult to obtain for highly dynamic systems such as intrinsically disordered proteins (IDPs) which must be described as structural ensembles. Here, we present IDPConformerGenerator, a flexible, modular open-source software platform for generating large and diverse ensembles of disordered protein states that builds conformers that obey geometric, steric, and other physical restraints on the input sequence. IDPConformerGenerator samples backbone phi (φ), psi (ψ), and omega (ω) torsion angles of relevant sequence fragments from loops and secondary structure elements extracted from folded protein structures in the RCSB Protein Data Bank and builds side chains from robust Monte Carlo algorithms using expanded rotamer libraries. IDPConformerGenerator has many user-defined options enabling variable fractional sampling of secondary structures, supports Bayesian models for assessing the agreement of IDP ensembles for consistency with experimental data, and introduces a machine learning approach to transform between internal and Cartesian coordinates with reduced error. IDPConformerGenerator will facilitate the characterization of disordered proteins to ultimately provide structural insights into these states that have key biological functions.
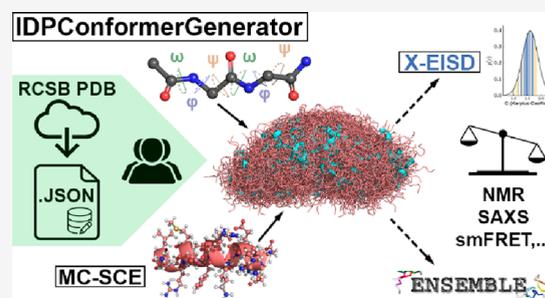
■ INTRODUCTION

Disordered states of proteins, including unfolded states, intrinsically disordered regions (IDRs) of otherwise folded domains, and full intrinsically disordered proteins (IDPs), are increasingly recognized for the roles that they play in folding kinetics,[1] aggregation propensity,[2,3] critical biological functions,[4] and pathological disease states.[5] Structural insights are needed to better understand these disordered protein states, and a variety of solution experiments have been developed to enable structural and dynamic descriptions of disordered proteins using nuclear magnetic resonance (NMR), small-angle X-ray scattering (SAXS), single-molecule fluorescence (SMF), and other data types.[6−11] However, solution experimental data for disordered states are averaged over a very large number of heterogeneous interconverting conformations, leading to greater challenges in structural interpretation than for folded proteins. Thus, specific computational approaches are required to bridge the gap between experiment and structural ensembles for disordered protein states.

The overall general approach begins with a large set of potential fractionally populated conformations and then selects a subset of these and/or assigns weights to conformational subpopulations that best agree with the available, but highly averaged, experimental restraints. These two components have typically been considered to be separate problems, and a number of methods exist for each. TraDES,[12,13] Flexible-meccano,[14] FastFloppyTail,[15] and other methods[16] are available to generate conformer pools, based primarily on the statistical distributions found in folded protein structures from the RCSB Protein Data Bank (PDB).[17,18] TraDES builds trajectories of three Cα positions at a time based on the probabilities in a set of nonredundant structures from the PDB and then fills in the rest of the chain. Flexible-meccano builds

chains by selecting φ/ψ torsion angles based on amino acid-specific conformational potentials derived from the PDB. FastFloppyTail also utilizes a three-residue fragment-based approach, with a bias toward the loop regions of the PDB. An approach from the group of Bernadó[16] similarly uses data from the PDB extracted as tripeptide segments. Another approach builds on Flexible-meccano but uses tripeptide conformers derived from molecular dynamics (MD) simulations.[19]

Because the structural ensembles provided by these methods are agnostic to experiment, a separate step is needed to select a subset of the conformations or, more generally, reweight the conformers in the pool to define ensembles that best represent information about the disordered state from the solution experiments. These include, among others, ENSEMBLE,[20] ASTEROIDS,[20,21] X-EISD,[22,23] BME,[24] and BW[25]/VBWSS,[26] with a number utilizing Bayesian statistics[22-24,27] and/or maximum entropy[24,28] to address inherent uncertainties in experiments and back-calculations from a disordered structural ensemble. MD simulations are an alternative to the statistical sampling of torsion angle pools, providing conformers that are biased by the physicochemical interactions included in the force fields[29-32] and represent Boltzmann weighted states. Furthermore, some MD approaches to generating IDP ensembles integrate experimental observables directly during the sampling phase. For example, some have used maximum entropy[33,34] and Bayesian statistics with averaged NMR biases[2,35] to guide the molecular dynamics sampling of IDPs toward conformations in better agreement with experimental data. Another uses fragments from MD simulations with a reweighted hierarchical chain growth algorithm[36] incorporating experimental data to generate disordered ensembles.

Together these approaches have all been valuable for both creating and ultimately characterizing a variety of disordered proteins; however, a number of challenges remain. In particular, for disordered proteins with a preferential sampling of fractional secondary structure and tertiary contacts, especially for longer sequences, the starting pool sample becomes the more limiting factor for the successful identification of subsets for reweighted ensembles that can fit experimental data. While a number of these tools can generate conformers biased by known secondary structure distributions, most of these tools are not flexible as to how users can generate disordered conformer ensembles as well as evaluate them with respect to experimental data.

Here, we report the open-source software platform IDPConformerGenerator to generate disordered protein conformations, utilizing a wide range of new and novel methods and models within a single software suite. IDPConformerGenerator begins with backbone builds based on torsion angle distributions of phi (φ), psi (ψ), and omega (ω) found in the PDB and then enables the building of side-chain ensembles using Monte Carlo side-chain entropy (MC-SCE) that completes the all-atom description by including hydrogens. IDPConformerGenerator has significant flexibility in user-defined options for the size of peptide fragments used to build the backbone, amino acid substitutions, secondary structure biases, steric clash criteria, and energy biasing using force fields. Additional stand-alone and integrated algorithms within IDPConformerGenerator extend the fundamental internal coordinate conformer ensemble builds with state-of-the-art transformations to Cartesian coordinates using Int2Cart,[37] which yields more correct valence geometries and reduces steric clashes. Finally, the generated ensembles can be evaluated with stand-alone and integrated software modules such as the X-EISD Bayesian model for assessing agreement with many different experimental data types including NMR, SAXS, and single-molecule fluorescence resonance energy transfer (smFRET).[22,23] What makes IDPConformerGenerator distinct from other tools is its flexibility as a user-friendly tool kit to explore different computational strategies and protocols for rationally defining conformational ensembles of (intrinsically) disordered protein sequences.

We demonstrate that IDPConformerGenerator can efficiently calculate ensembles of proteins of up to at least 440 residues in length with a variety of secondary structure distributions and tertiary contact patterns. Many of these have reasonable root-mean-squared deviations (RMSDs) from experimental solution data, particularly some generated with bias for fractional secondary structure based on NMR chemical shifts. These results support the utility of IDPConformerGenerator for the creation of initial conformer pools that are more physically representative and more readily optimized by using experimental restraints with X-EISD[22,23] or ENSEMBLE.[20]

■ METHODS

Design of IDPConformerGenerator. We set out to design a tool to efficiently generate conformers that realistically sample the likely conformational space of intrinsically disordered sequences from the statistical sampling of backbone torsion angles (φ, ψ, and ω) of short protein segments in the PDB that are identical or similar in sequence to the protein under investigation. This led to our choice to exploit the PDB for the sampling of torsion angle space to generate more physically meaningful conformers, a choice also utilized by TraDES,[12,13] Flexible-meccano,[14] FastFloppyTail,[15] and others. Given these physically sound backbone conformations, we also provide side-chain building algorithms such as MC-SCE that can generate ensembles of different rotamer states that are Boltzmann weighted and further all-atom representations by including hydrogens. The resulting sets of conformations are intended to be utilized as inputs to downstream approaches to define ensembles that best agree with experimental data, such as those that select subsets (e.g., ENSEMBLE[20] and ASTEROIDS[20,21]), reweight conformers (e.g., BME[24]), or both (X-EISD[22,23]).

Building Conformational Ensembles. IDPConformerGenerator starts by creating a protein sequence database annotated with φ, ψ, and ω torsion angles and secondary structure per residue. We use nonredundant lists of structures such as those generated by the Dunbrack PISCES database.[38] Hence, IDPConformerGenerator builds structures by extracting φ, ψ, and ω backbone torsion angles from the database, fragment-by-fragment (with fragments being peptides of variable length), using torsion angles matching the input sequence for each fragment or matching a user-defined residue tolerance (or substitution) dictionary. While other tools utilize rigid fragment sizes, IDPConformerGenerator allows users to configure the size and probability of the peptide fragments used to build the IDP chain stepwise, modulating the sampling strategy to explore. IDPConformerGenerator uses DSSP nomenclature[39,40] to annotate residues by secondary structure elements. Because of this, users can define the secondary structure classes that IDPConformerGenerator will sample, either across the sequence or in a residue-specific manner, based on knowledge such as from NMR chemical shifts for fractional populations of secondary structures as a function of
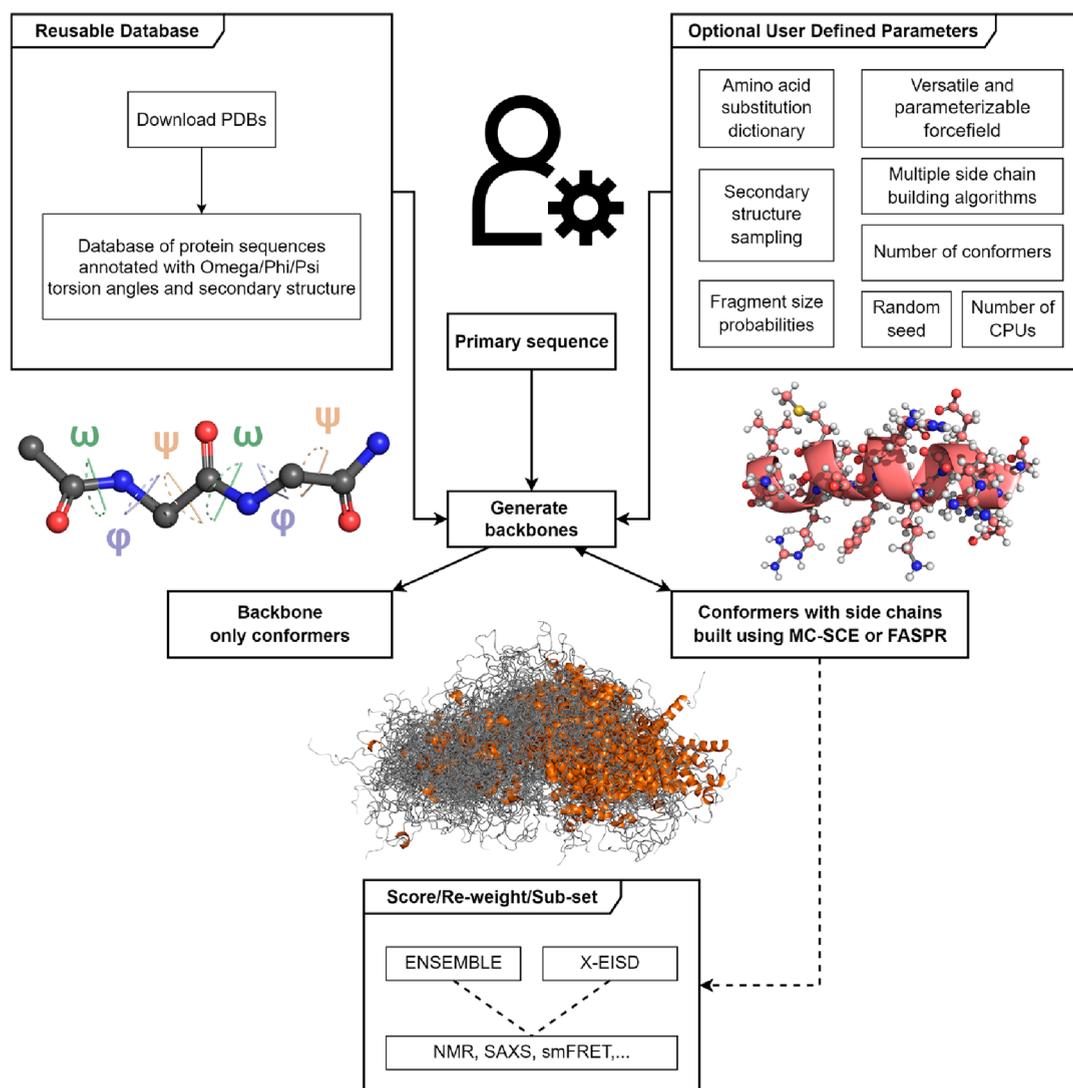
Figure 1. Schematic diagram of the IDPConformerGenerator approach. Generating conformers requires the creation of a reusable database of backbone torsion angles and input of the primary sequence, with optional user-defined parameters including those for amino acid substitutions, secondary structure sampling, and fragment size probabilities. An example of a peptide of 2 residues (fragment size 2) that is used to build inhibitor-2 (I-2) is shown with backbone torsion angles labeled, a helical secondary structure with all-atom side chains of an I-2 conformer, and an illustrative set of 100 generated conformations of I-2. Conformers that are generated can then be scored or reweighted based on experimental data.

residue.[41−43] We provide several methods to sample bond geometries when converting from internal to Cartesian coordinates. The most important one is the Int2Cart methodology[37] that predicts bond lengths and angles for a set of torsion angles and residue identities. Instead of using hard spheres to model atom volumes, IDPConformerGenerator computes the whole Lennard-Jones (L-J) potential to tolerate small clashes that can be compensated for by favorable interactions, with user-defined thresholds to direct the acceptance of a fragment or backtracking to rebuild. To generate full side chains, IDPConformerGenerator has integrated the MC-SCE algorithm, originally developed for the more difficult case of folded proteins but which works easily for disordered states.[44]

Associated and Integrated Tools. IDPConformerGenerator is designed as a platform to facilitate the generation of disordered protein conformations, including analysis of resulting ensembles and scoring or reweighting with respect to experimental data. Tools for the analysis of structure are integrated within IDPConformerGenerator, including those for secondary structure, torsion angle distributions, radius of gyration (R_g), end-to-end distances, asphericity (deviation from the spherical shape of the conformers), and $C\alpha−C\alpha$ distance and distance-difference matrices. The software easily enables the use of downstream tools for scoring, reweighting, or subsetting to fit experimental data and will serve as a future platform for integrating these tools, including the simple ENSEMBLE approach and the X-EISD Bayesian model.

IDPConformerGenerator Software Platform. To facilitate its development and use, IDPConformerGenerator is open source and extensively documented and the architecture is modular to allow easy extension with other modules and strategies (https://github.com/julie-forman-kay-lab/IDPConformerGenerator). IDPConformerGenerator is written in Python, and all of its automated functionalities are available as command line commands. In addition, all of IDPConformerGenerator's functionalities are available through the Python interpreter and can be imported and used
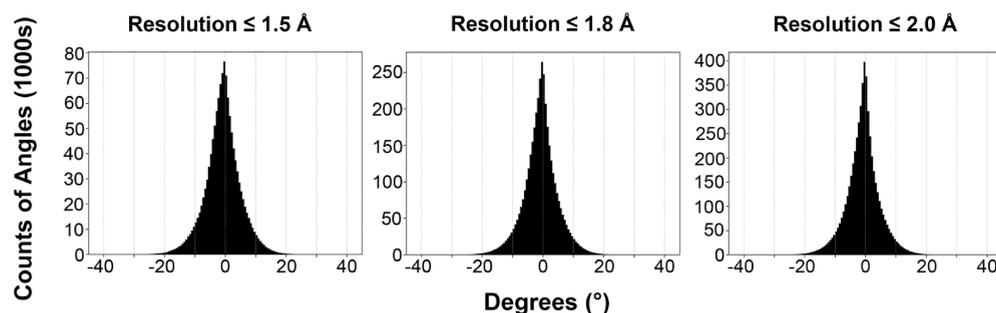
Figure 2. Histogram of ω dihedral angle distributions for structures found within the IDPConformerGenerator database. PDBs from the 24 003 PDB structure database were used, with sets of this with resolutions better or equal to 1.5 Å (∼5000 structures), better or equal to 1.8 Å (∼16 000 structures), and better or equal to 2.0 Å (full set). The deviations from an ω torsion angle of 180° (trans) are plotted, centered around 0°, to facilitate the visualization of the distribution rather than the actual ω angles. Cis peptide bonds are ignored for visualization purposes.

independently by more advanced users. Also, all IDPConformerGenerator pipelines are distributable across multiple CPU cores. IDPConformerGenerator's software design facilitates a flexible approach to building conformers with numerous user parameters that enable very different realistic ensembles to be built, with the design philosophy and options discussed here. The overall workflow of IDPConformerGenerator is described in detail next and is schematized in Figure 1.

Backbone Conformer Generation. IDPConformerGenerator requires a torsion angle database from which to build backbone conformers. Users can provide custom-made lists of the PDB chains to assemble the torsion angle database, thus allowing tuning for resolution and diversity. IDPConformerGenerator considers only continuous chains and selects the atoms with the highest occupancy for those with alternative locations. The IDPConformerGenerator parser works with both the older PDB format and newer mmCIF files. For the results reported here, we employed a fixed nonredundant database of PDB structures from the Dunbrack PISCES database[38] (Oct 15, 2020), including high-resolution structures with resolution better than or equal to 2.0 Å and an R factor of ≤0.25 with a maximum mutual sequence identity of 90%.

Conformer backbones are built fragment-by-fragment, where fragments can be configured for different lengths (described below). Physical validation of the conformers (for example, a steric clash check) is parametrizable via force fields and threshold parameters. If a clash is found, then IDPConformerGenerator will delete the last fragment and attempt a new one. If no new fragment can be added without a steric clash, then the building process will backtrack to delete additional fragments. This process is repeated until the whole backbone is complete. With the default parameters, some sequences can be built very fast while others require extensive sampling times, also dependent on length (see below).

Including the Peptide Bond ω Torsion Angle. One of the major differences between IDPConformerGenerator and previous backbone sampling tools is that IDPConformerGenerator includes peptide ω torsion angles in the sampling and building regime. The ω torsion angle is considered to be part of the torsion angle set for each residue in the order $\omega/\varphi/\psi$. The decision to include ω is fundamental to our strategy to explore the IDP landscape by the addition of multiple residue-sized fragments, and since ω angles can vary to up to 20° in loop regions of high-resolution structures (Figure 2), including ω in the generator increases the accuracy of the extracted fragment. Note that this variation is not dependent on the resolution of the structure but that helices have a narrower ω

torsion angle distribution (Supporting Information Figure 1). Accurate ω torsion angles are also critical for the future incorporation of folded domains within otherwise disordered chains.

Sequence Specificity of Chosen Torsion Angles. IDPConformerGenerator builds structures based on extracting backbone torsion angles from the torsion angle database, using torsion angles either (i) only from residues that exactly match the input sequence (when possible; see below) or (ii) from residues that match user-defined residue substitutions, i.e., isoleucine matching either isoleucine or leucine. The ability to explore a narrow or broader sequence space of the PDB with user-defined flexibility is an important feature of IDPConformerGenerator. Utilizing the exact sequence to find torsion angles in the PDB-derived database will guide IDPConformerGenerator to choose torsion angles that reflect the structural biases of that sequence. This capitalizes on the PDB-derived database as an "empirical force field" and is expected to generate local and secondary structure biases based on the sequence dependence of these structures. Enabling the substitution of residues for similar residues, with a user-defined substitution list, recognizes the availability limits of exact sequence matches in the PDB and extends the potential torsion angles possible to be sampled.

IDPConformerGenerator has the ability to extract substitution lists based on a table derived from the EDSSMat50 IDP-specific substitution matrix[45] (Supporting Information Table S1A), with the user specifying the columns to be used to define how conservative or liberal to make the substitutions. Users can also provide specific substitution lists through the command line (with an example shown) '-subs {"A": "AG"}', with substitutions described in the form of a Python dictionary where keys are the residues to replace and values are the list of residues to include.

Peptide Fragment Sizes. IDPConformerGenerator enables users to define the size and probability of the peptide fragments used to build the IDP chain stepwise, modulating the sampling strategy to explore. By default, IDPConformerGenerator samples fragment sizes of one, two, three, four, and five residues with 10, 10, 30, 30, and 20% probabilities, respectively. Users can freely configure these values in any given manner. Therefore, IDPConformerGenerator can emulate previously published algorithms that build conformer chains by single residue or tripeptide additions while allowing selection using countless other strategies. Shorter fragments (such as one residue at a time) disregard the sequence context of residue torsion angle frequencies, while with larger fragment

sizes, information about cooperative structure (helical, turn, or extended strand-like elements) from the PDB is included in the growing disordered protein chain. In practice, fragment sizes of up to pentapeptides are most valuable because it is hard to find sequence matches for longer segments, and cooperative structures found in disordered proteins generally do not extend beyond five residues (although there can be regions of a longer cooperative helix). If a sequence match for the requested fragment size is not found, then IDPConformerGenerator reduces the fragment size, one residue at a time, until a sequence match is found in the database, taking into account residue substitutions. Fragments are reduced until single residue additions are sampled. Regardless of the size of the fragment, if a proline residue in the input sequence follows the selected fragment, then IDPConformerGenerator tries to expand the fragment sequence to include the proline as well because prolines impose severe torsion restraints on preceding residues, a strategy used by other disordered chain-generating tools.[16,46,47]

Secondary Structure Sampling. IDPConformerGenerator uses DSSP nomenclature[39,40] and the IDPConformerGenerator-created torsion angle database can be configured to annotate residues by DSSP or any other third-party software (via the IDPConformerGenerator ʹsscalcʹ interface) that classifies secondary structure elements. Because of this, the secondary structure classes of the PDB database that are sampled can be defined by users. A logical approach for generating disordered ensembles is to sample the loop regions of folded structures, which dominate most IDPs/IDRs. FastFloppyTail focuses on these regions, and others have noted an increased ability to fit local structural experimental data to ensembles derived from the coil or loop regions of PDBs,[48] even though these regions can be poorly defined.[49] Using loops will bias to irregular structural elements found in the PDB that most likely represent disordered states and will also include short helical and extended elements. However, significantly populated helical elements and other secondary structure elements are found in disordered proteins states, so other DSSP codes are valuable to include. Therefore, IDPConformerGenerator allows users to sample any residues regardless of secondary structure annotation ("ANY" flag) or to specifically sample loops, helices, extended structures, poly proline II helices, or an individual or combination of any DSSP secondary structure code.

The secondary structure bias can be performed uniformly across the sequence or in a residue-specific manner, using knowledge such as from NMR chemical shifts for fractional populations of secondary structures as a function of residue.[41−43] Depending on user choice, IDPConformerGenerator can prioritize building with the secondary structures of interest over the full sequence, leading to sampled fragments consisting only of residues matching a single secondary structure annotation, or can completely disregard secondary structures while building to allow the inherent secondary structure propensities observed in the PDB database to emerge. In this way, for example, ABC could be a fragment in which A and B residues are annotated as a loop and C is annotated as a helix (with C being the first residue of a helix following a loop). Moreover, custom secondary structure sampling based on experimental knowledge of the fractional populations of secondary structures can be used, which can in turn override the database bias to build conformers to match known structural probabilities. For the bias of secondary

structure on a per-residue basis, building utilizes a custom secondary structure sampling database file containing fractional propensities for different secondary structures as a function of residue derived from NMR chemical shift data (using cssconv with δ2D[42] or CheSPI[43]). If the chemical shift data are not available but other knowledge of sampling of helical or extended/β-strand regions exists (or if users want to explicitly define these), then users can specify where significant sampling of helical or extended/β-strand regions occurs and sample the rest of the conformer without bias. Combining the rich ability to sample torsion angles from specific secondary structure annotations with the residue-type substitutions that increase the matching tolerance and specification of fragment sizes, users can sample highly restrictive or very broad conformational spaces.

Side-Chain Building. During the backbone building process immediately after each backbone fragment is created, alanine side chains are added to all residues, except for glycines and prolines for which the full residue is added. These dummy alanines serve as coarse-grained representations of the real side chain. They avoid building backbone conformations that are too compact to fit side chains without steric clashes, yet the volume of the alanine side chain is small enough to allow the backbone to sample packed conformations, enabling the exploration of side-chain packing.

However, full side chains must be added, and IDPConformerGenerator adds side chains using the MC-SCE algorithm by sending backbone atom coordinates only and excluding any alanine and proline side chains. The MC-SCE algorithm is a Monte Carlo approach to building side-chain conformations on a predefined backbone structure[44] that utilizes a convergent Rosenbluth sampling scheme and an augmented Dunbrack library for side-chain rotamer sampling.[44] The MC-SCE algorithm was originally written in Fortran but was fully rebuilt in Python to interface with IDPConformerGenerator to build side-chain structures. Given a backbone structure, MC-SCE builds the side chains by aligning the backbone N, C_α and C' atoms of the Dunbrack templates with the backbone from IDPConformerGenerator. The side chains are then rotated according to the sampled torsion angles, and this sampling procedure is the key to the Monte Carlo nature of the algorithm.

MC-SCE can be used both as a stand-alone option (https://github.com/THGLab/MCSCE) and as two modes for working within IDPConformerGenerator. The simple mode provides an option for rapidly adding side chains to a backbone structure without introducing clashes, but the conformations might be energetically suboptimal. Conversely, the exhaustive mode generates side-chain conformations via the user-defined total number of trials for the parallel execution of the building process, with the all-atom structure having the lowest energy of these returned to IDPConformerGenerator, but takes longer to run. (See the Supporting Information for more details.)

The FASPR[44] algorithm used to build side-chain structures is also an integrated option. This stand-alone software for side-chain packing performs quickly for folded proteins. Note that FASPR does not include hydrogens, leading to a need to identify an optimal approach to build them afterward. We have opted for MC-SCE as our preferred approach because it generates a complete all-atom description of conformers, including hydrogens, which is an important advantage over FASPR.

Internal to Cartesian Coordinate Transformations. The design of IDPConformerGenerator as a builder based on torsion angle sampling, rather than based on Cartesian coordinate space, has benefits and drawbacks. One clear benefit is that building with secondary structure biases, such as from NMR chemical shifts and backbone ^3J-coupling data, is "native" to the builder. Building with tertiary contact biases, such as from NMR $^1H-^1H$ NOE or PRE data, is not. Importantly, energy calculations are made on Cartesian coordinates. In order to facilitate energy calculations, the conformers based on internal coordinates must be back-transformed to Cartesian coordinates.

The original approach used for most of the work reported here uses statistical sampling of bond angles for the set of matched fragments and average values for bond lengths based on the identity of the previous residue and the one following the residue being built. The currently recommended approach that improves upon the aforementioned strategy uses Int2Cart developed by Li and co-workers,[37] which is a deep learning model that better predicts the correlations among the whole sequence and the bond lengths and bond angles for a given set of ω, φ, and ψ torsion angles to yield more accurate Cartesian coordinates. This very recent implementation can be used as a stand-alone option (https://github.com/THGLab/int2cart) and is also integrated within IDPConformerGenerator directly.

Energy Considerations. Instead of using hard spheres to model atom volumes, IDPConformerGenerator computes the whole Lennard-Jones (L-J) potential to create conformers that are self-avoiding polymers. The default L-J parameters are the Amber14SB force field, which were used for the results generated here but are also user-definable. Computing the whole L-J potential allows the building engine to tolerate small clashes that can be compensated by favorable interactions and compensates for the fact that rigid conformers are created; i.e., no flexible minimization is performed at any stage. Severe clashes will, nonetheless, have a profound impact on the energy term, and thus the energy threshold for rejection can be defined by users, with higher values allowing the exploration of broader conformational space. This feature is useful when modeling sequences with reduced representations in the database.

IDPConformerGenerator can build backbone-only or full side-chain-containing conformers. For this reason, two energy threshold parameters are implemented: one to control the tolerance for backbone atoms ("-etbb") and another to control the energy threshold in all-atom conformers with side chains ("-etss"). The energy thresholds to accept or reject a conformer can be calculated pairwise (atom-by-atom) or over the full structure based on user choice. For each fragment built, the energy is computed; if it is below the threshold, then the fragment is accepted, otherwise it is rejected. If side chains are being built, then once the backbone is complete, IDPConformerGenerator attempts to place the side chains. If successful (the energy term is below the threshold), then the conformer is saved. Otherwise, the backbone conformation is considered to be too restrictive to build side chains, the whole conformer is discarded, and the creation of a new conformer starts. Since the energy threshold for acceptance after side chain addition is distinct from the threshold controlling backbone building, a user can accept all side-chain packing results by providing a large number for the side-chain energy threshold.

X-EISD Bayesian Model. IDPConformerGenerator is designed as a platform and supports the direct incorporation of the calculated ensemble into downstream tools for scoring and reweighting based on experimental data. The internal integration of these tools is envisioned in the near future. Of particular interest is X-EISD,[22,23] a method which calculates the maximum log likelihood of a protein structural ensemble by accounting for the uncertainties in a wide range of experimental data and back-calculation models from structures. These data include NMR chemical shifts, J couplings, residual dipolar couplings (RDCs), hydrodynamic radii, nuclear Overhauser effects (NOEs), and paramagnetic resonance enhancements (PREs); smFRET; and SAXS curves.[22,23] We have also introduced new data types, NMR R_2 relaxation rates and S^2 order parameters, for the selection of an IDP ensemble consistent with NMR dynamics data.[50] Given the ensembles created with IDPConformerGenerator, the X-EISD model can be used as a scoring function to reweight the IDP ensembles for the best agreement with experimental data based on the different experimental and back-calculation uncertainties.

Analysis Tools. There are a number of commands currently integrated within IDPConformerGenerator that can enable the analysis of resulting ensembles. These include the analysis of the resulting fractional secondary structure. In addition, a set of complementary analysis tools were utilized to ask specific research questions regarding the ensembles (see below; available as stand-alone scripts). These include the RMSDs from experimental data restraints and ENSEMBLE and X-EISD scores; pairwise RMSDs of atomic coordinates; measures of local structure, including secondary structure and $\varphi/\psi/\omega$ distributions; measures of hydrodynamic properties, including R_g, end-to-end distances, and asphericity (deviation from spherical shape of the conformers); and measures of tertiary contacts, including the $C\alpha-C\alpha$ distance and distance difference matrices.

Additional User-Defined Parameters. Parameters are available to control reproducibility, including random seeds. IDPConformerGenerator runs are deterministic; i.e., the same results can be achieved by providing the same initial database, the same input parameters, and the same random seeds on the same machine. Users can also specify the number of cores of a multiprocessor computer to use.

■ RESULTS

In order to demonstrate the utility of IDPConformerGenerator and ask questions regarding the optimal parameters for building diverse and physically meaningful ensembles, we have used a set of intrinsically disordered proteins (IDPs) of various sizes: Sic1,[51] α-synuclein,[52] inhibitor-2,[53] and Tau,[54] as well as the unfolded state of the N-terminal SH3 domain of the *Drosophila* signaling protein Drk (drkN SH3).[55]

- Sic1 is a yeast cell-cycle regulator that inhibits a cyclin-dependent kinase and is degraded following ubiquitination due to binding the ubiquitin ligase substrate-binding domain (Cdc4 WD40 domain) in a dynamic complex dependent on multisite phosphorylation.[51] The N-terminal 92 amino acids (aa) of Sic1 are necessary and sufficient for binding and have been extensively characterized by NMR, SAXS, and smFRET, and this fragment is therefore used here.[6,56−58]

- Human α-synuclein (aSyn, 140 aa) is highly abundant in the brain, where it is found largely in the axon terminals
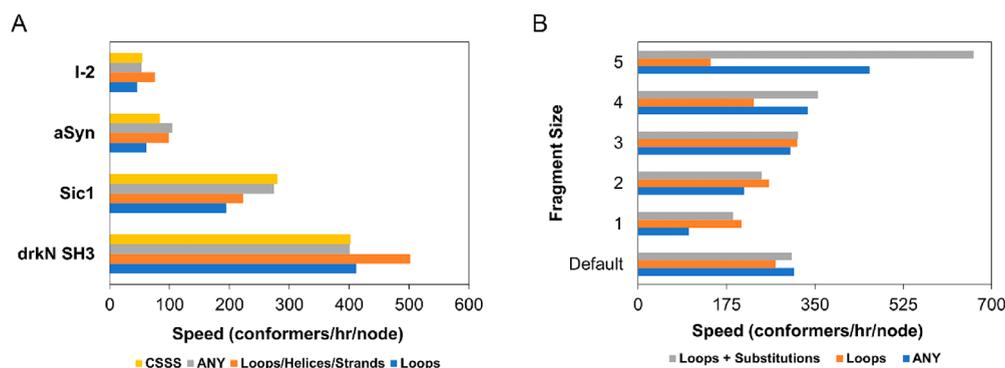
Figure 3. Timings for IDPConformerGenerator with MC-SCE and dependencies on the protein test system (size), secondary structure sampling, and fragment length. Speed is defined as the number of conformers per hour. (A) Speeds for variable secondary structure sampling methods on disordered proteins with different lengths, shown for sampling with custom secondary structure propensities (CSSS, yellow), "ANY" secondary structure (gray), combinations of loops, helices, and strands (orange), and only loops (blue). Speeds are shown for selected ensembles of the drkN SH3 domain unfolded state (59 amino acids, aa), the Sic1 N-terminal targeting region (92 aa), α-synuclein (aSyn, 140 aa), and inhibitor 2 (I-2, 159 aa). Speeds for all conformer ensembles generated including for the Tau fragment (441 aa) are in Supporting Information Table S2A. (B) Speeds for variable fragment sizes and secondary structure sampling methods for Sic1 are shown for sampling with only loops with substitutions (gray), only loops without substitutions (orange), and "ANY" secondary structure (blue). Default fragment length probabilities are 0.1, 0.1, 0.3, 0.3, and 0.2 for fragment lengths of 1, 2, 3, 4, and 5, respectively.

of presynaptic neurons to regulate synaptic vesicle trafficking and subsequent neurotransmitter release.[52] In the presence of membrane vesicles (or other lipid environments), α-synuclein forms a helical structure, but in the absence of lipid, it is highly disordered with a minimal propensity for helical or other secondary structure. It has been studied in both states, but for testing purposes, we utilize NMR and SAXS data from the disordered state.[15,21,59−64]

- Inhibitor-2 (I-2, 159 aa) is an inhibitor of protein phosphatase 1 (PP1), forming a dynamic complex with PP1 that orders only a limited portion of I-2 upon binding, based on crystallographic data.[53] In the absence of PP1, I-2 is disordered yet has a significant population of helices, based on characterization by NMR.[65,66]

- Tau (microtubule-associated protein tau) is a 758-residue IDP with numerous functional annotations, including the promotion of microtubule assembly and stability and roles in establishing and maintaining the polarity of axons in neurons.[54] It is an RNA-binding protein that phase separates in vitro and is found in cellular biomolecular condensates, consistent with its lower complexity sequence.[67] We use the first 441 residues as a test system since a fragment encompassing these residues has been studied using NMR.[68,69] Short Tau peptides have also been studied,[15] and we similarly utilize a Tau peptide as a test system.

- Finally, the drkN SH3 domain exists in dynamic equilibrium between folded and unfolded states, with the unfolded state extensively studied as a model disordered protein for the development of ensemble calculation methods due to the large number of experimental NMR, SAXS, and smFRET restraints available and its small size (59 aa).[22,50,66,70]

Sequences for these proteins and fragments are given in Supporting Information Table S1B. Note that there are some peptide sequences of aSyn and Tau in the PDB database we use (Supporting Information Table S1C), many in complex with antibodies. It may be valuable to include structures of the protein of interest or homologous proteins, such as complexes

of folded proteins with the disordered protein of interest (or its fragments), to provide conformations that are likely to be sampled at some level. Alternatively, users may choose to exclude such structures to avoid potential bias. Either approach is possible because IDPConformerGenerator allows users to assemble custom-made databases of torsion angles from user-defined input PDB lists. The number of sequence matches for different fragment sizes of the drkN SH3 domain in our database for different secondary structure sampling, including exact matches or with substitutions, is given in Supporting Information Table S1D to provide concrete examples of how torsion angles are chosen in IDPConformerGenerator. The 'stats' subclient calculates the sequence matches in the database for an input sequence and considering the input parameters of the building process. In this way, users can easily assess the number of angles available for each chunk and identify possible bottlenecks where residue tolerance might be needed.

Here we characterize multiple aspects of IDPConformer-Generator: computational speed for generating ensembles, the diversity of conformer sampling, the presence or absence of secondary structure (especially helical fraction), how well these unoptimized disordered ensembles recapitulate experimental data, and comparisons to other structural ensemble generators including TraDES, FastFloppyTail, and MD simulations.

Computational Timings. The speed of conformational ensemble generation is important, particularly for larger proteins, as large and conformationally diverse input pools are valuable for further reweighting or subsetting. We compared speeds for generating disordered conformers using IDPConformerGenerator with different fragment sizes and different secondary structure options for all of the test systems. For these, we generated backbones for each protein with a 100 kJ backbone energy threshold and used MC-SCE for side chains. The goal was to yield 1000 successful full conformers for each protein such that timings were normalized on a per successful conformer basis. Exact timings and the percentage of successful conformers from the generated backbones can be found in Supporting Information Table S2A.

Figure 3A demonstrates the general trend of faster conformer generation for shorter chains, as expected, with a
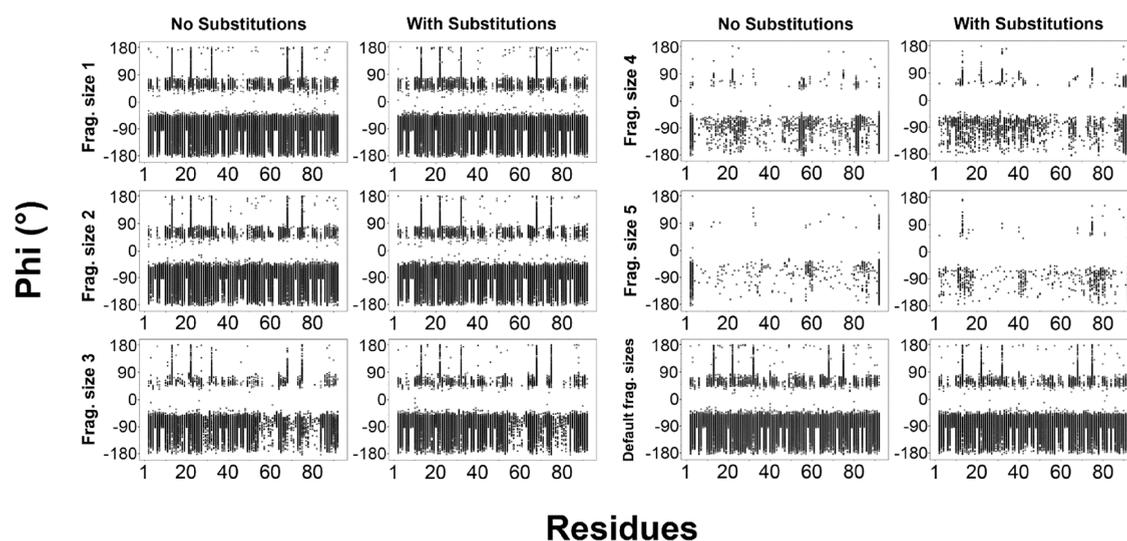
Figure 4. Phi (φ) torsion angles in Sic1 ensembles sampled using different fragment sizes, with and without substitutions. Calculations were for 1000-conformer ensembles generated by sampling loops only, with fragment sizes of 1, 2, 3, 4, and 5 and default fragment size probabilities. The left and right columns are for the Sic1 sequence without and with substitutions, respectively. Substitutions are derived from columns 5, 3, and 2 of the EDSSMat50 amino acid substitution matrix. The plot was generated with the '--plots' flag in the 'idpconfgen torsions' CLI.

nonlinear dependence. Building with only helices or extended strands is usually faster than building with loops or mixtures of loops with helical or extended structures, such as with CSSS or ANY, as loops increase the likelihood of steric clashes and difficulties in side-chain packing, although helices and strands are not as representative of disordered states (Supporting Information Table S2A). As shown in Figure 3B, increasing the fragment size significantly increases the speed of conformer generation for the proteins investigated, and varying the secondary structure sampling method alters the speed for different fragment sizes. In most cases, using substitutions was also found to be faster, likely due to more fragment matches in the database. Overall, conformer generation is reasonably efficient but strongly dependent on chain length, with speeds of 400−500 conformers per hour per computer node for the drkN SH3 domain unfolded state (59 aa), 200−275 for Sic1 (92 aa), 50−100 for aSyn (140 aa), 40−75 for I-2 (159 aa), and about 5 for Tau (441 aa) using one node on the Graham supercomputing resource. For this and all other calculations unless otherwise specified, we used one node of the Graham resource of Compute Canada (now Digital Research Alliance of Canada) with 2x Intel E5-2683 v4 Broadwell @ 2.1 GHz CPUs and with 125 GB of RAM per node.

We also tested the intersection of the impact of sequence length and the diversity of amino acid residues in the sequence on the speed of conformer generation. Low-complexity IDRs using fewer amino acids are increasingly understood to play a functional role in facilitating phase separation within biomolecular condensates or membraneless organelles.[71,72] Of our test proteins, the Tau fragment is the longest (441 aa) and is known to phase separate.[67] It is also lower in complexity than the other test proteins, with the first 300 residues annotated as having compositional bias by CAST and being low complexity by SEG, respectively.[73,74] Such low-complexity sequences are not found in the folded proteins in our database, and we explored if they would take longer to build. We quantified the speed of conformer generation in minutes per amino acid on the multiprocessor server. Tau was segmented into 3 segments of 147 aa to compare with I-2 (159 aa) and

aSyn (140 aa) and 5 segments of ~90 residues in order to compare with Sic1 (92 aa). We found that the central 147-residue segment of the Tau fragment was the fastest to build but that there were no clear trends on the basis of complexity when comparing Tau to aSyn or I-2 (Supporting Information Figure S2).

The side-chain addition step is much longer than backbone generation, with our preferred side-chain packing algorithm MC-SCE taking a larger fraction of the time as the chain length increases. MC-SCE was initially optimized for packing side chains onto the backbone of folded proteins. Although the success rate decreases with longer backbone lengths, we found that the settings in MC-SCE could be optimized for IDPs by reducing the number of attempts/trials spent on packing side chains onto backbones from 128 to 32. For Tau, using 32 trials increased the speed per conformer by 3 to 4.4 times depending on secondary structure sampling (Supporting Information Table S2B). Another observation based on these benchmarks is that the success rate increases with an increased number of backbone conformers available as input to MC-SCE.

For methodological purposes, we also asked about the optimal energy flags for the speed of calculation of conformers that do not have significant steric clashes in order to facilitate the rapid building of structural ensembles. We built sets of 1000 backbone conformers of I-2 with loops or other secondary structure sampling with either 100 or 250 kJ pairwise energy thresholds and used MC-SCE for side chains, with average times of 68 and 38 min, respectively. The ~80% increase in time for the 100 kJ threshold led to only an ~10% gain in clash-free conformers. We observed similar results for aSyn, with average times of 45 and 25 min, respectively, and an ~80% increase in time for the 100 kJ threshold and only an ~15% gain in clash-free conformers. Thus, increasing the energy threshold can speed up the full conformer generation time for proteins at least as long as I-2 (Supporting Information Table S2C).

Sampling Depth. Next, we interrogated the depth of the torsion angle space in ensembles built from torsions derived from the PDB data set. When building proteins with a specific
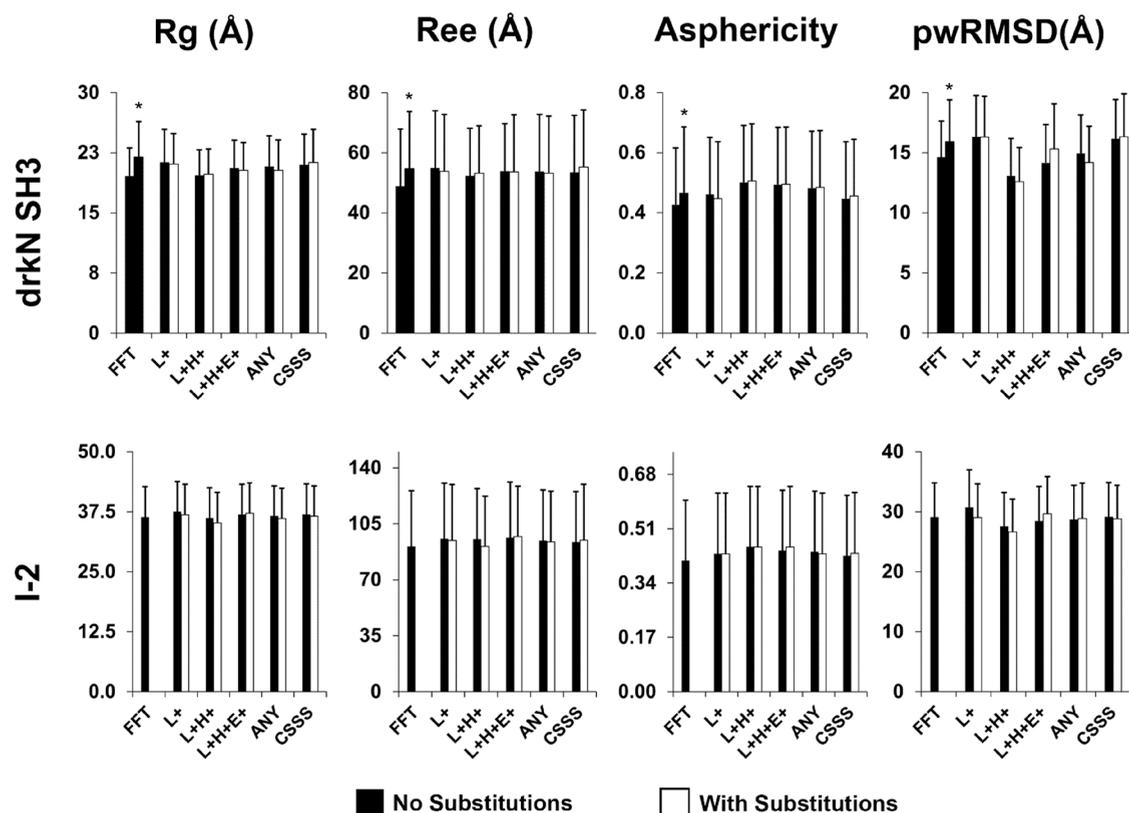
Figure 5. Diversity analysis of conformational ensembles of the drkN SH3 domain unfolded state and I-2. The radius of gyration (R_g), end-to-end distance (R_{ee}), asphericity (A), and pairwise root-mean-squared deviations of atomic positions (pwRMSDs) are shown as a function of secondary structure sampling parameters for 1000-conformer ensembles generated with different secondary structure sampling, including loops (L+), loops and helices (L+H+), loops, helices, and extended strands (L+H+E+), and all torsion angles agnostic to secondary structure (ANY) and biased by δ2D chemical shifts (CSSS) or with FastFloppyTail (FFT) for the drkN SH3 unfolded state (row 1) and I-2 (row 2). Standard deviations for R_g, R_{ee}, A, and pwRMSD are also shown as bars. Supporting Information Figure S6 shows similar data for other protein systems. * is for the standard FFT protocol, which for this case treats the protein as a mixture of ordered and disordered, while the other is for a modified protocol in which the protein is considered to be fully disordered.

sequence, particularly for fragment sizes of 3, 4, and 5, the finite size of the PDB-derived database leads to minimal torsion angle options as only sequence matches of the defined fragment size can be used to build. This leads to what we call torsion angle bottlenecks for specific residues. Figure 4 shows the φ distributions for Sic1 generated using loops with various fragment sizes, demonstrating decreasing numbers of distinct torsion angles as the fragment size increases. For fragment sizes of 5 between residues 20−30, essentially 1 set of backbone torsion angles was used over all of these 1000 structures. Supporting Information Figure S3 shows histograms of how many segments of the drkN SH3 domain sequence for various fragment sizes are present in the database, demonstrating the minimal data for fragment sizes of 6 and 7, with values also provided in Supporting Information Table 1D. In order to avoid such torsion angle bottlenecks, mixtures of fragment sizes are optimal when requesting exact sequence matches. The default of probabilistic sampling of fragment sizes of 1, 2, 3, 4, and 5 in a ratio of 1:2:3:3:1 enables contributions from larger fragment sizes with cooperative structural elements while minimizing torsion angle bottlenecks, as seen in the bottom right rows of Figure 4. Using substitutions can help avoid bottlenecks, with Figure 4 panels reporting on ensembles with substitutions showing greater torsion angle coverage than for those without. Increasing the number of DSSP codes utilized can also be beneficial (Supporting Information Figure S4), as

using only helices or only strands yields limited torsion angle sampling (and is not realistic for disordered chains). Being agnostic to secondary structure annotation is another approach, as seen for the difference between using loops only or all possible annotations for the drkN SH3 domain sequence (Supporting Information Figure S5).

We then looked for the optimal parameters (fragment size, secondary structure flags) for increasing diversity of calculated structures, as measured by average pairwise RMSDs, hydrodynamic parameters, and asphericity. R_g, the end-to-end distance (R_{ee}), and asphericity are all measures of the shape of a conformation, with smaller R_g and R_{ee} values and asphericity approaching 0 implying more spherical, compact chains while large values reflect irregular, less compact shapes. As expected, we note that it is critical to incorporate loop regions to build diverse structural ensembles of disordered protein states; with only helical or extended DSSP flags, long helices or strands are built, which are not representative of disordered conformations (Figure 5, Supporting Information Figure S6, and Supporting Information Table S3). This is seen by the much higher R_{ee} and asphericity values, such as for those built with helices only having asphericity values of >0.8 and with strands only having R_{ee} values 1.5 to 2 times as large as for those built with loops. To further increase the diversity of calculated structures, the "ANY" secondary structure flag is optimal as it will use the natural secondary structure
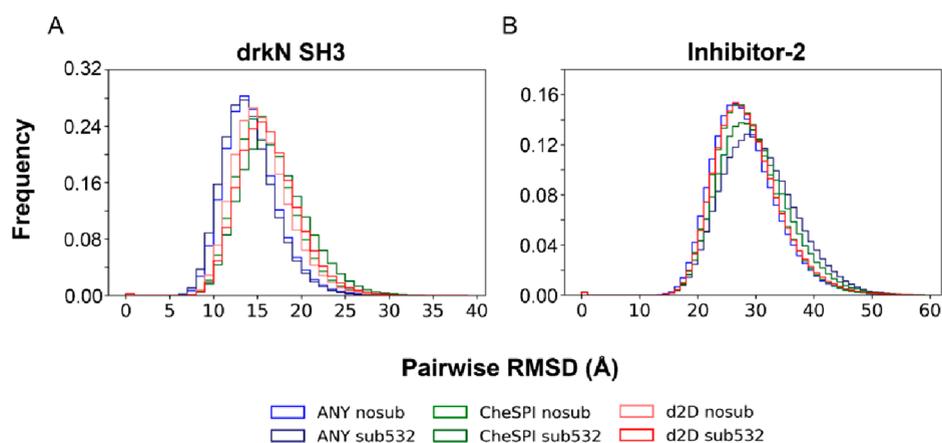
Figure 6. Pairwise RMSD distributions for ensembles of the (A) drkN SH3 domain unfolded state and (B) I-2. Calculations were for different ensembles of 1000 conformers each, plotted with bin sizes of 5 Å. "ANY" indicates sampling the database without biasing secondary structures, "nosub" indicates no substitutions, "sub532" indicates amino acid substitutions from columns 5, 3, and 2 of the EDSSMat50 amino acid substitution matrix, and "CheSPI" or "δ2D" indicates custom secondary structure sampling (CSSS) pools biased by CheSPI or δ2D estimations of secondary structure propensities.
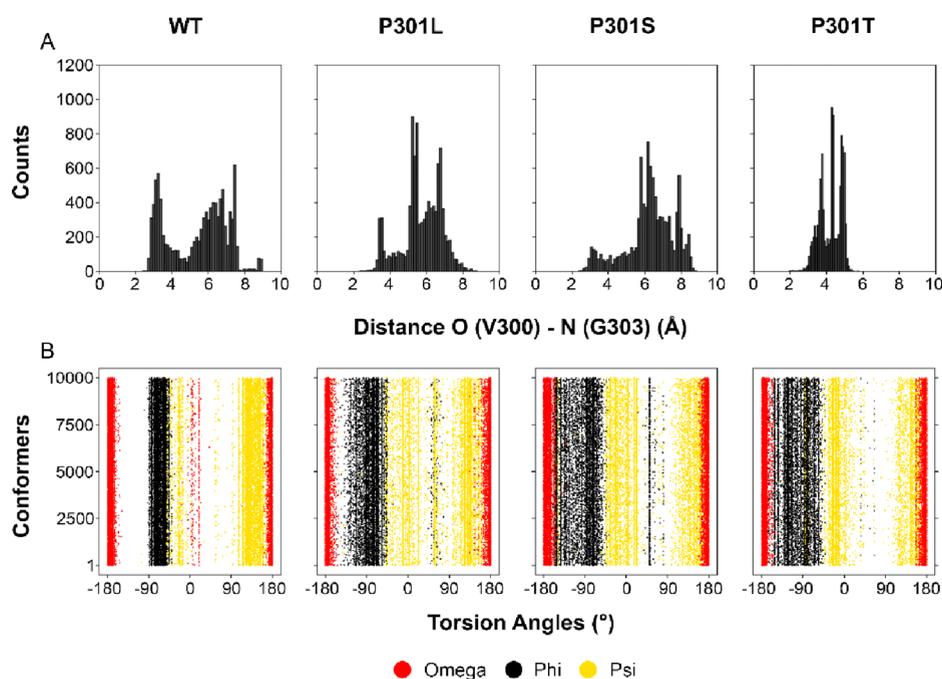

Figure 7. Local structural variations between the Tau K18 16-mer WT and different mutants. (A) Distribution of the distance between V300 O and G303 N atoms in 10 000-conformer ensembles generated with no substitutions. (B) Torsion angle distributions for position 301 of the different conformers in these WT and mutant ensembles, with ω representing the torsion angle N-terminal to the φ, as is our convention (typically denoted as ω of the preceding residue).

propensities of the entire PDB database and will not be limited to user-defined secondary structures that restrict the sampling of conformational space (see below).

Plotting pairwise RMSDs as a distribution (Figure 6) demonstrates that the ensembles are smoothly sampled, with no significant clusters of similar structures, consistent with our goal of generating diverse conformers. Varying secondary structure sampling approaches can also increase the variety of conformational space explored, as the custom secondary structure sampling shifts the RMSD histogram to larger values. As seen in plots of pairwise RMSD distance matrices (Supporting Information Figure S7), no regions of lower pairwise RMSDs are seen, indicating that the generated conformers have a large variability in Cα backbones. Pairwise

RMSD is correlated to protein length, with RMSD values ranging from above 5 Å to 30 Å for the shorter disordered drkN SH3 domain unfolded state (59 aa) and from 15 Å to above 50 Å for I-2 (159 aa), indicating significant heterogeneity in conformational sampling.

We were also interested to see if IDPConformerGenerator is able to effectively capture local structural changes with amino acid sequence changes. We used a 16-mer peptide from the Tau K18 fragment previously studied by Stelzl and co-workers; reweighted hierarchical chain growth was used to generate Tau ensembles recapitulating structural details that were identified by NMR to have microtuble binding capacity and that are lost upon mutation of position P301.[36] To investigate the conformational diversity explored by IDPConformerGenerator
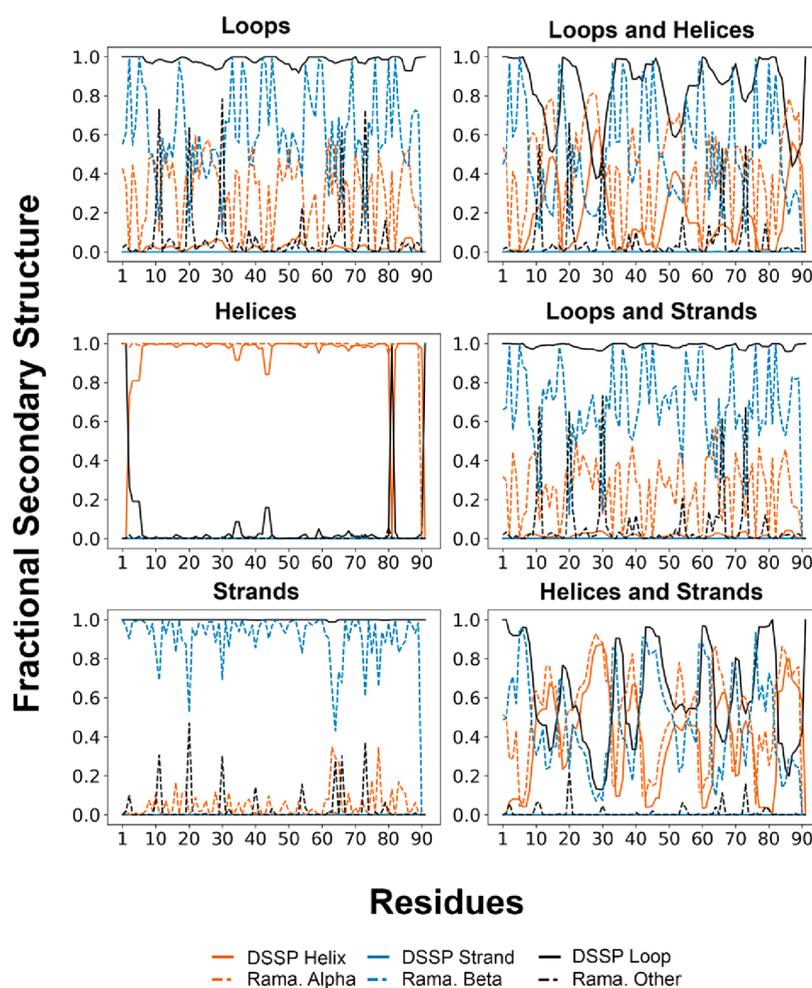
Figure 8. Fractional secondary structure in Sic1 ensembles. Analyses were performed on 1200-conformer pools of Sic1 generated with different combinations of secondary structure sampling consisting of loops, helix, and extended strands. Orange indicates α-helix detected by DSSP (solid) and the α-region on the Ramachandran (Rama.) diagram (dashed). Blue indicates extended strand for DSSP (solid) and the β-region on the Ramachandran diagram (dashed). Black indicates coil/loop for DSSP (solid) and other regions on the Ramachandran diagram (dashed).

and the variation in conformations for single-site mutations, we generated sets of 10 000 conformers for wild type (WT), P301L, P301S, and P301T for the Tau fragment sequence: DNIKHVP^{301}GGGSVQIVY. We sampled by considering only sequence matching, disregarding secondary structure annotations, and allowed no residue substitutions for sequence matching.

One of the structural parameters explored in the Stelzl study is the distance between V300 O (backbone carbonyl oxygen) and G303 N (backbone amide nitrogen). Figure 7A shows distributions for this O−N distance for the different variants. In agreement with the Stelzl study, we observe a considerable fraction of conformers for the WT with distance below 4 Å, reflecting a turn structure and likely hydrogen bond, while for mutants these occurrences are much rarer. Each mutant reveals different patterns of O−N distances, showing that IDPConformerGenerator can capture local conformational diversity from single-point mutations and that these will be incorporated into the larger disordered chain. Figure 7B shows the torsion angles for residue 301 in the variants. Here, we also observe very different profiles. Note the presence of conformers with a *cis*-prolyl peptide bond for P301 reflecting the natural tendency of *cis*-Pro in the context of this sequence but absent in the mutants lacking proline. These results demonstrate that

IDPConformerGenerator can effectively sample realistic local conformations in a sequence-specific manner, consistent with its design. Another approach to sampling particular turn types or other structures that is available with IDPConformerGenerator is to utilize an amino acid substitution dictionary to incorporate residues with known propensities for these structures.

Fractional Secondary Structure. An obvious question regards the impact of the secondary structure flags on the ultimate fractional secondary structures in the ensembles built. We generated 1200-conformer ensembles of Sic1 using different combinations of secondary structure sampling with loops (activated by default), helices, and strands. IDPConformerGenerator can pool together DSSP codes T (hydrogen-bonded turn), S (bend), B (β-bridge), P (PPII helix), I (pi-helix) and ' ' (blank, loops/irregular) as loop (L), H (α-helix) and G (3-10 helix) as helix (H), and only E (extended strand, participating in β-ladder) as strand (E). For all of our calculations, we utilized this pooled set of DSSP codes. We generated Sic1 ensembles due to its lack of inherent significant biases in secondary structure propensity[56,57] (Figure 8). When restricting to loops only or loops and strands, similar sampling is observed with greater sampling of the β-region of the Ramachandran diagram, but since there are no hydrogen-
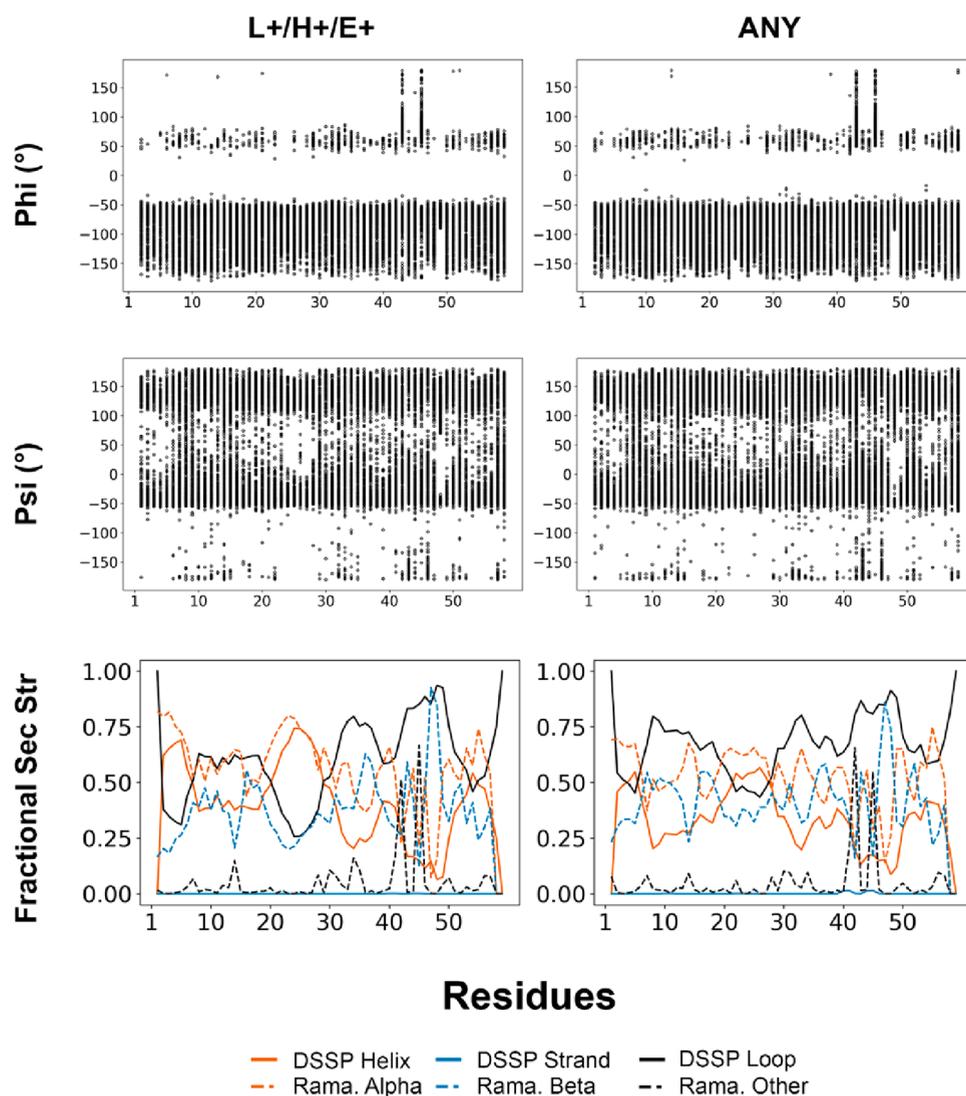
Figure 9. Comparison of torsion angle sampling for L+/H+/E+ and ANY. Ensembles of 1000 conformers each of the drkN SH3 domain unfolded state were generated with sampling a combination of loops (L), helix (H), and extended strands (E) or sampling without biasing secondary structure with the ANY flag. Phi and psi (φ and ψ) torsion angle distributions for each conformer pool are shown as a scatter plot in the first two rows. The third row depicts fractional secondary structure based on DSSP (dark solid lines) or the Ramachandran (Rama.) diagram (dashed lines), with orange indicating α-helix for DSSP and the α-region of the Ramachandran diagram, blue indicating extended strand for DSSP and the β-region of the Ramachandran diagram, and black indicating coil/loop for DSSP and other regions of the Ramachandran diagram.

bonded interactions, DSSP catalogs these as loops. There is also significant sampling of the α-region and some small amounts of cooperative helix are observed. With strands only, sampling of the β-region of the Ramachandran diagram is dominant, with no strands defined by DSSP, again due to the lack of hydrogen bonds. Restricting sampling to helices, however, leads to dominant sampling of the α-region of the Ramachandran plot, and as expected, these structures show significant α-helix as defined in the DSSP. With loops and helices, there are also significant cooperative helices generated. Similar results were seen for the drkN SH3 unfolded state (Supporting Information Figure S8).

Sampling with all three secondary structure options in combination (loop, helix, strand) is not the same as sampling with the ANY flag ('--dany'), as the latter approach samples based solely on the sequence matching patterns, disregarding secondary structure annotations, thus reflecting the inherent structural propensities of the input sequence fragments as

present in the database. The explicit listing of secondary structure codes limits to sampling fragments with the same secondary structure code for all residues while with the ANY flag this is not a requirement, so we wondered if there would be significant differences in emerging structural patterns. An analysis of ensembles of the drkN SH3 domain unfolded state demonstrates no significant visual differences in torsion angle distributions, but the ANY pools do have greater psi ranges between residues 22 and 29 and there are greater helical propensities for the LHE pool compared to the ANY pool (Figure 9). Although the general trends of secondary structure propensities seem similar between the LHE and ANY pools, small differences demonstrate that these options generate different conformer pools. We recommend the ANY flag to build IDP conformer ensembles with the sampling of torsion angles based on frequencies observed in the PDB. To maximize the sampling of torsion angle space, we recommend
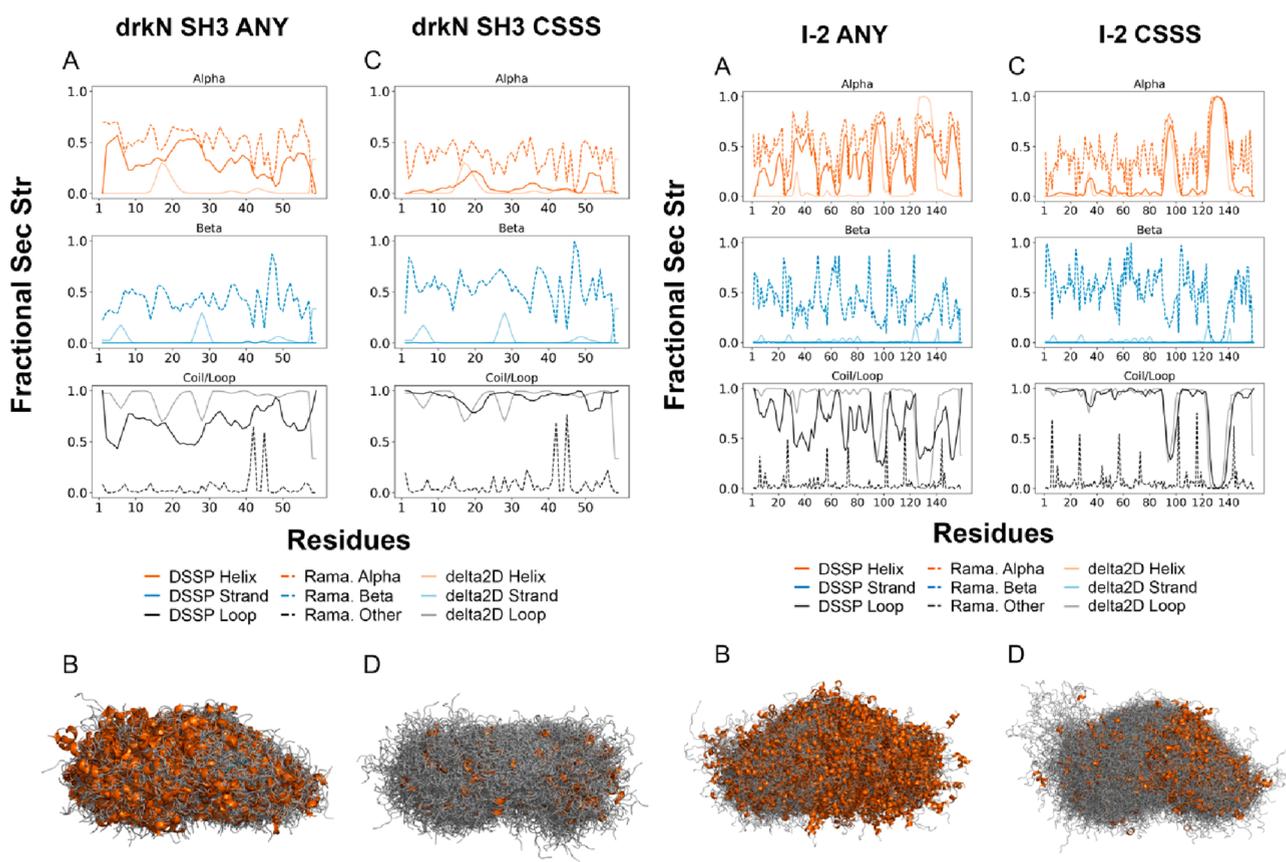
Figure 10. Custom secondary structure sampling. (Left) For the drkN SH3 domain unfolded state, two sets of 3000 conformers each were generated, and (right) for inhibitor-2 (I-2), two sets of 1500 conformers each were generated, with (A, B) the "ANY" flag or with (C, D) the CSSS flag to do custom secondary structure sampling based on δ2D calculations from NMR chemical shift data. (A, C) Plots of fractional secondary structure based on DSSP (dark solid lines), the Ramachandran (Rama.) diagram (dashed lines), or δ2D (light solid lines). Orange indicates α-helix for δ2D and DSSP and the α-region on the Ramachandran diagram. Blue indicates extended strand for δ2D and DSSP and the β-region on the Ramachandran diagram. Black indicates coil/loop for δ2D and DSSP and other regions on the Ramachandran diagram. (B, D) Aligned conformers of the ensembles using PyMOL.

sampling with both ANY and LHE to minimize torsion angle bottlenecks.

Importantly, we were interested in whether our design of IDPConformerGenerator to exploit the secondary structure propensities found in the PDB would match experimentally measured propensities from NMR chemical shifts. Two sets of 3000 conformers each of the drkN SH3 domain unfolded state were generated using a backbone energy threshold of 100 kJ, with the "ANY" flag and with the CSSS flag to do custom secondary structure sampling based on δ2D[42] calculations from NMR chemical shift data[75] on a per-residue basis. As seen in Figure 10 (left), there are natural secondary structure propensities for α-helix, particularly for residues 16−29, based on δ2D predictions for secondary structure propensities.[42] At residues 58 and 59, the predicted probabilities of secondary structure are set to 1/3 as no chemical shift data are available. Although extended β-strand regions have also been predicted with δ2D, DSSP defines extended strands based on both torsion angle ranges (the same ones as used for segmenting the Ramachandran space) and hydrogen bonds, and there are minimal cases of tertiary contacts satisfying β-hydrogen bonds in these disordered ensembles. However, sampling in the β-region of the Ramachandran diagram is plentiful. (Note that it may be valuable to utilize a different definition of strand pairing besides DSSP that is more permissive for local

backbone geometries to characterize potential β-strands.) This ensemble shows that helical structure is oversampled relative to what is found experimentally. However, the regions where significant α-helical secondary structure is sampled do overlap with the observed secondary structure propensities identified by δ2D. With custom secondary structure sampling, in contrast, there is very good agreement for the α-helical and coil/loop structure on a per-residue basis with that suggested by δ2D (Figure 10, left). Sampling in the β-region is somewhat increased, with no observed β-strand H-bonding structure seen using DSSP. Overall, biasing the sampling for torsion angles in the PDB based on secondary structure yields an ensemble with an overestimate of helical structure compared to the δ2D estimates, while directing the sampling by NMR data, as expected, yields an ensemble in much closer agreement to these data.

Similar results were found for I-2, which has significantly populated helices around residues 85−99 and 121−145, based on NMR chemical shifts[75] with δ2D assignments. These peaks match with sampling from the α-region of the Ramachandran plot in the ANY ensemble (Figure 10, right), but there is significant helical structure throughout. Biasing by the NMR data, we can generate an ensemble with nearly exact agreements of the secondary structure propensities calculated by δ2D to the secondary structure propensities of the
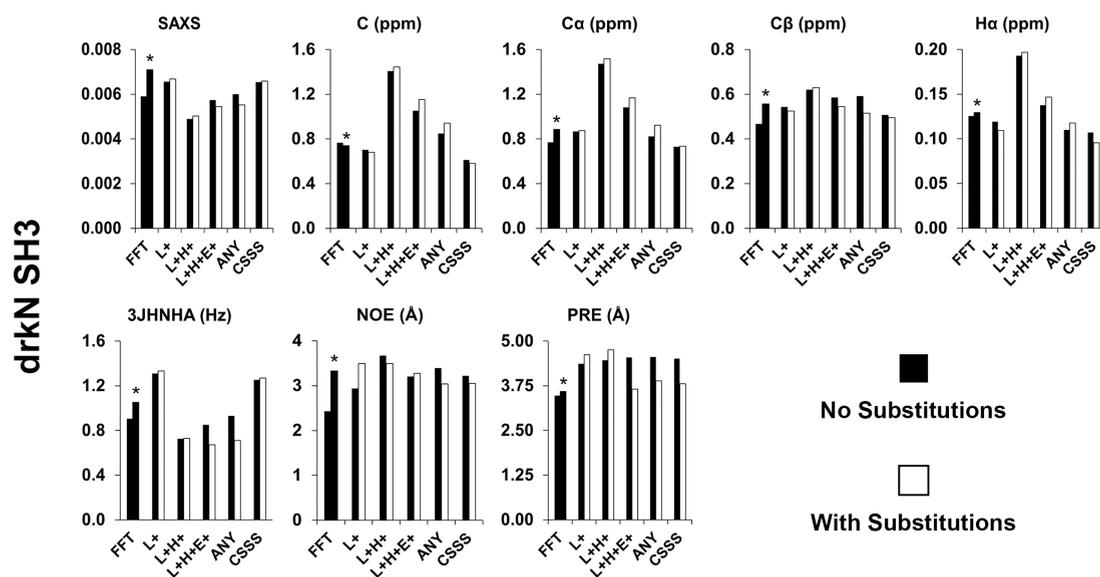
Figure 11. Root-mean squared deviations (RMSDs) of back-calculated values from conformational ensembles to experimental data for the drkN SH3 domain unfolded state. Analyses of 1000-conformer ensembles generated using various secondary structure sampling and using FastFloppyTail (FFT). RMSDs are given for SAXS, chemical shifts (carbonyl, Cα, Cβ, Hα), PRE, $^3J_{HN-HA}$, and NOE if available. Sources of experimental data are provided in Methods. * is for the standard FFT protocol, which for this case treats the protein as a mixture of ordered and disordered, while the other is for a modified protocol in which the protein is considered to be fully disordered.
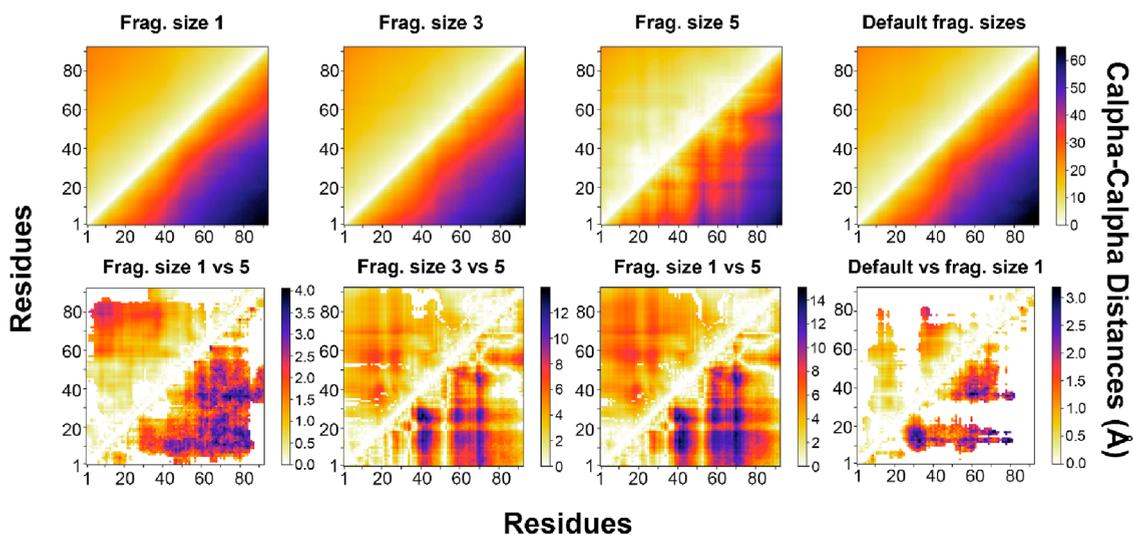

Figure 12. Analysis of tertiary contacts for Sic1 ensembles. (Top row) Cα−Cα distance matrices (lower) with deviations (upper) for 1000-conformer ensembles of Sic1 generated with the loops-only flag for secondary structure, with substitutions from columns 5, 3, and 2 of the EDSSMat50 amino acid substitution matrix and with variable fragment lengths. (Bottom row) Significant differences between Cα−Cα distance matrices (lower) and deviations (upper) ($P < 0.05$ from a Mann−Whitney U test).

conformer ensemble calculated by DSSP (Figure 10, right). While sampling torsion angles in the PDB using the ANY flag may provide some insight into the natural propensities for α- or β-regions of the Ramachandran diagram, biasing the sampling based on experimental NMR data can yield conformer pools that are more likely to be representative of the disordered protein. Additional plots of residue-specific fractional secondary structures for calculated ensembles are provided in Supporting Information Figures S9−S12.

Comparison with Experimental Data. Beyond the chemical shift-derived secondary structure, we were interested in the ability of the generated ensembles to match experimental data. While the goal is to build diverse conformer pools that have the potential to fit experiment following a

subsetting or reweighting procedure, such as with ENSEMBLE[20] or X-EISD,[22,23] an initial match to experiment clearly demonstrates this potential. Using RMSD from experimental data (Figure 11 and Supporting Information Figure S13) and ENSEMBLE and X-EISD scores as metrics (Supporting Information Table S4), we found that IDPConformerGenerator ensembles are not in very close agreement with the experimental data, as expected, but that the deviation is not large for many restraint types, such as SAXS, chemical shifts, 3-bond $^1HN−^1Hα$ J couplings, and RDCs. While there are larger deviations for those representing tertiary contacts, PREs and $^1H−^1H$ NOEs, it is difficult to directly compare the RMSD values for the different experimental data types as the range of data varies considerably. An RMSD of ∼4 Å for PRE, a

measurement that goes out to 20 or 30 Å, may be closer than an RMSD of ∼0.8 ppm of Cα chemical shifts, a measurement that varies less than 2 ppm. CSSS generally provides ensembles in better agreement with Cα and Cβ chemical shift restraints, as expected, particularly for proteins with known significant sampling of secondary structure, such as I-2.

A significant measure of the ability to match experimental restraints is the effective sampling of various tertiary contacts. A comparison of the Cα−Cα distance matrices for fragment sizes of 1, 3, and 5 as well as the default fragment size sampling for Sic1 shows that there is a relatively smooth sampling of longer distances (Figure 12, top row). Significant differences are observed between ensembles generated with the three different fragment sizes, as seen in the difference distance matrices between ensembles, demonstrating that mixtures of fragment sizes are valuable for sampling a diverse set of tertiary contacts (Figure 12, bottom row). In addition, there are significant differences in tertiary contacts for Sic1 ensembles generated with loops and with "ANY" (Supporting Information Figure S14). Together, these results provide evidence that using a large, combined input pool of conformations created with varying fragment sizes, secondary structure sampling, and other parameters would enable reweighting or subsetting to fit the distance restraint and other data types.

Comparison to Other Disordered Chain-Generating Tools. One of the early motivations for building IDPConformerGenerator is the significant number of steric clashes found in TraDES[12,13] conformers. The definition of a clash depends on whether only the repulsive portion of the L-J potential is considered or the whole L-J potential is used, allowing closer distances which are compensated for by favorable interactions. We generated a set of 1000 Sic1 conformers using default TraDES parameters and used Chimera to check for steric clashes[76] using a stringent criterion based largely on distance (similar to the repulsive portion of the L-J). With criteria of no backbone clashes and ≤5 side chain clashes, this TraDES ensemble had no conformers meeting the criteria. In contrast, 1000-conformer IDPConformerGenerator ensembles of Sic1 built using custom secondary structure sampling and default fragment sizes had 324/1000 conformers meeting these criteria. A similar drkN SH3 domain unfolded state pool had 395/1000 conformers meeting these criteria. Chimera's clash definition is more stringent than the one we utilize in IDPConformerGenerator and MC-SCE, which allows close contacts if compensated for by favorable L-J energy, thus all of these IDPConformerGenerator conformers are arguably physically realistic conformations. IPDConformerGenerator does generate many more conformers with fewer steric clashes as defined by Chimera than does TraDES.

We also calculated a set of FastFloppyTail[15] ensembles to enable comparison with IDPConformerGenerator. While there are different parameters for running FastFloppyTail, it is not user customizable in terms of sampling specific secondary structures or various fragment lengths, with the exception of using 3-mer and/or 9-mer fragment libraries. We therefore used the recommended protocol for each system, with 3-mer fragment libraries and with an additional run to force the drkN SH3 domain to be disordered throughout. (See the Supporting Information for details.) We measured the speed, diversity, sampling of secondary structure, and match to experimental data (Figures 5 and 11, Supporting Information Figures S6 and S9−S13, and Supporting Information Tables S2, S3, and S4). For the quantitative speed comparison, we considered only the

time of the calculation following setup with the initial files. For IDPConformerGenerator, initial setup includes the generation of the initial torsion angle database, which we needed to do only once for all of the systems, and provides the specific protein sequence with input parameter files. Generating the initial torsion angle database took 37 min on a desktop computer using 63 of the 64 cores, 20−30 min for downloading, while processing and generating the database were fast. The time is very dependent on the Internet connection speed and number of cores since the process is embarrassingly parallel. For FastFloppyTail, there is no ability to define multiple processors, and there are a number of steps and files required before the conformer generation process, including the prediction of disordered regions and secondary structure and creating a fragment library, which is required for each protein. The predictions require multiple external websites or programs. For the test systems, we could utilize the premade files on the FastFloppyTail website, but for other proteins, this would not be the case. For the drkN SH3 domain, Sic1, aSyn, and I-2, the fragment libraries took between 11 and 16 min each to calculate on the HPC system that we used for ensemble generation, while for Tau it was about 45 min (Supporting Information Table S2). Another issue with FastFloppyTail is that disordered proteins that are not predicted to be disordered can yield challenges in setup. In particular, the unfolded state of the drkN SH3 domain has a sequence that is not predicted to be disordered, leading to our testing both the recommended algorithm and one defining it as disordered (Supporting Information). α-Synuclein is known to fold into a long α-helix in the presence of lipid or micelles and different predictive algorithms have variable success in predicting its disordered state,[77] and the authors of FastFloppyTail noted a need to find a predictor which correctly identified its disordered state.[15]

The results demonstrate that IDPConformerGenerator is faster than FastFloppyTail for chains shorter than 200 residues with default parameters. There is generally minimal difference in the diversity of the ensembles between the two tools, although asphericity values are higher for IDPConformerGenerator and FastFloppyTail ensembles are often more compact. The secondary structure sampling for FastFloppyTail ensembles often falls between IDPConformerGenerator ANY and CSSS biased by NMR chemical shifts, with FastFloppyTail having higher populated secondary structure than suggested by experiment. Matches to experimental data are more variable, with IDPConformerGenerator run using different secondary structure sampling approaches giving the lowest RMSD values for different data types for different systems, often lower than the FastFloppyTail ensemble, particularly for the CSSS with chemical shifts, although not always. A clear distinction is that IDPConformerGenerator enables users to flexibly define different approaches for the generation of conformers, including for diversifying the resulting ensembles.

To compare an alternative strategy of IDP conformer ensemble generation, we have extracted conformers from MD trajectories generated using an optimized force field from Robustelli et al.[78] (See Supporting Information, Additional Methods, for details.) We compared the three overlapping protein systems with ours (drkN SH3, Sic1, and aSyn) from this MD study, calculating fractional secondary structure profiles (Supporting Information Figures S15−S17) and agreement with experimental data (Supporting Information Table S4A). As seen in Supporting Information Figures S15−

S17, ensembles from these MD simulations deviate from δ2D[42] predicted secondary structure propensities, while IDPConformerGenerator's CSSS approach can easily recreate any secondary structure profile, including δ2D calculated propensities, while maintaining diversity. The agreement of IDPConformerGenerator conformers with experimental data is in general comparable to that of these MD simulations using an optimized force field for disordered proteins (a99SB-*disp*),[78] even showing better agreement in some cases (Supporting Information Table S4A). IDPConformerGenerator, with its significantly lower computational cost than the MD, facilitates the calculation of multiple ensembles with various secondary structure sampling approaches. This includes CSSS, which usually leads to better agreement with chemical shift data than the MD conformers. Different IDPConformerGenerator secondary structure sampling approaches also enable comparable or better fits than MD to other data. Interestingly, the drkN SH3 IDPConformerGenerator ensembles have significantly better agreement with the PRE and NOE data than the MD conformers, while for Sic1 the MD fits better to PRE data. Overall, IDPConformerGenerator performs very well compared to MD trajectories generated with the a99SB-*disp* force field.

DISCUSSION AND CONCLUSIONS

A range of theoretical and computational approaches for generating disordered ensembles exist,[10,79] each of which has strengths and unique features based on the design philosophy. Testing of IDPConformerGenerator on our set of model disordered proteins demonstrates that this tool is highly flexible and can function as a platform to enable the generation of various initial conformational pools built with different biases and parameters, which is valuable for addressing a range of scientific needs. It is computationally efficient depending on the sequence length and parameters and can enable sampling using the frequencies of secondary structures within the PDB database provided or the experimental secondary structure propensities from NMR experiments. The resulting ensembles are not far from fitting experimental data, including those for local structure, tertiary contacts, and overall hydrodynamic properties. IDPConformerGenerator ensembles have agreement with experiment comparable to those generated by MD simulations, at significantly less computational cost. Ensembles generated with the various secondary structure sampling approaches have distinct levels of agreement with the multiple experimental restraint types, suggesting that each IDPConformerGenerator build configuration samples unique regions of conformational space. Future work will explore the optimal parameters for sampling structures to facilitate the identification of subsets or reweighting to best fit restraints, including tertiary contacts. However, the current results strongly suggest that using an input pool with a combination of ensembles generated with different approaches, including with and without substitutions, varied fragment sizes and combinations, and varied secondary structure sampling including bias with NMR chemical shift-derived probabilities, can effectively sample a range of conformational space to facilitate fitting experimental data with subsets or reweighting.

Scientific software is often created by scientists and not software engineers, leading to tools that are not as user-friendly, generalizable, easy to maintain, or thoroughly documented as desired. A larger goal of developing IDPConformerGenerator was to design it to be easy to use

so that it would be widely used, not only to generate disordered protein ensembles as starting pools for subsetting or reweighting but also to enable it to function as a platform for adding existing functionality or future approaches to define ensembles that best fit experimental data, for computational experiments testing various ideas, and for analyses of resulting ensembles. There are a number of straightforward extensions of IDPConformerGenerator planned, including the ability to build disordered regions around a folded domain, an important functionality (and one that motivated the creation of FastFloppyTail). Due to IDPConformerGenerator's modularity, analysis tools can easily be built utilizing current functions. Currently available functions include those to analyze ensembles for fractional secondary structure and torsion angle distributions and to analyze the database for the number of available sequence matches and for identifying structures with select keywords. Further additions, such as the analysis of tertiary contacts, could be implemented with ease and are planned for a future release. More significantly, this platform is being developed to include back-calculators for comparison to experimental data and Bayesian scoring and reweighting approaches such as X-EISD.[22,23] We envision that IDPConformerGenerator will be the basis for an expanding platform of tools to facilitate the structural characterization of IDPs and IDRs consistent with solution experimental data. We hope that our goal of developing a user-friendly and flexible platform will draw more researchers to the field of intrinsically disordered protein structural characterization, which in one view should be almost half the size of the folded protein structural biology community, given the relative amounts of disorder and folded structure in eukaryotic proteomes ($\sim$0.35 to 0.65).[4] Ultimately, the resulting structural ensembles should provide physical insights into how these abundant and dynamics states regulate and carry out their critical biological functions and how disease variants in IDPs/IDRs lead to pathology.

ASSOCIATED CONTENT

ⓢ Supporting Information

The Supporting Information is available free of charge at https://pubs.acs.org/doi/10.1021/acs.jpca.2c03726.

Supplementary tables (XLSX)

Analysis scripts (zip file with Python. py files) (ZIP)

IDPConfGen supplementary information (PDF)

AUTHOR INFORMATION

Corresponding Authors

João M. C. Teixeira − *Molecular Medicine Program, Hospital for Sick Children, Toronto, Ontario M5G 0A4, Canada; Department of Biochemistry, University of Toronto, Toronto, Ontario M5S 1A8, Canada;* Present Address: Bijvoet Centre for Biomolecular Research, Faculty of Science, Department of Chemistry, Utrecht University, Padualaan 8, Utrecht 3584CH, The Netherlands; Email: joaomcteixeira@gmail.com

Julie D. Forman-Kay − *Molecular Medicine Program, Hospital for Sick Children, Toronto, Ontario M5G 0A4, Canada; Department of Biochemistry, University of Toronto, Toronto, Ontario M5S 1A8, Canada;* ⓞ orcid.org/0000-0001-8265-972X; Email: forman@sickkids.ca

Authors

Zi Hao Liu − *Molecular Medicine Program, Hospital for Sick Children, Toronto, Ontario M5G 0A4, Canada; Department of Biochemistry, University of Toronto, Toronto, Ontario M5S 1A8, Canada;* ⊙ orcid.org/0000-0002-8357-8507

Ashley Namini − *Molecular Medicine Program, Hospital for Sick Children, Toronto, Ontario M5G 0A4, Canada*

Jie Li − *Pitzer Center for Theoretical Chemistry and Department of Chemistry, University of California, Berkeley, California 94720, United States;* ⊙ orcid.org/0000-0002-4727-1786

Robert M. Vernon − *Molecular Medicine Program, Hospital for Sick Children, Toronto, Ontario M5G 0A4, Canada;* Present Address: Amgen Inc. Research and Development, Burnaby, British Columbia V5A 1 V7, Canada.

Mickaël Krzeminski − *Molecular Medicine Program, Hospital for Sick Children, Toronto, Ontario M5G 0A4, Canada*

Alaa A. Shamandy − *Molecular Medicine Program, Hospital for Sick Children, Toronto, Ontario M5G 0A4, Canada; Department of Computer Science, University of Toronto, Toronto, Ontario M5S 2E4, Canada;* ⊙ orcid.org/0000-0001-7074-437X

Oufan Zhang − *Pitzer Center for Theoretical Chemistry and Department of Chemistry, University of California, Berkeley, California 94720, United States*

Mojtaba Haghighatlari − *Pitzer Center for Theoretical Chemistry and Department of Chemistry, University of California, Berkeley, California 94720, United States;* Present Address: Pfizer Inc., 610 Main Street, Cambridge, Massachusetts 02139, United States.

Lei Yu − *Pitzer Center for Theoretical Chemistry and Department of Chemistry, University of California, Berkeley, California 94720, United States;* ⊙ orcid.org/0000-0003-0159-1968

Teresa Head-Gordon − *Pitzer Center for Theoretical Chemistry, Department of Chemistry, Department of Chemical and Biomolecular Engineering, and Department of Bioengineering, University of California, Berkeley, California 94720, United States;* ⊙ orcid.org/0000-0003-0025-8987

Complete contact information is available at:
https://pubs.acs.org/10.1021/acs.jpca.2c03726

Notes

The authors declare no competing financial interest.

ABBREVIATIONS

aa, amino acids; aSyn, α-synuclein; CSSS, custom secondary structure sampling; drkN SH3, unfolded state of the N-terminal SH3 domain of Drk; E, DSSP code for extended strand participating in β-ladder; FFT, FastFloppyTail; H, pooled DSSP codes for α-helix and 3-10 helix; I-2, inhibitor-2; IDPs, intrinsically disordered proteins; IDRs, intrinsically disordered regions; L, pooled DDSP codes for hydrogen-bonded turn; bend, β-bridge; PPII helix, π-helix and loops/irregular structure; L-J, Lennard-Jones; MD, molecular dynamics; MC-SCE, Monte Carlo side-chain entropy; NMR, nuclear magnetic resonance spectroscopy; PDB, Protein Data Bank; PP1, protein phosphatase 1; SAXS, small-angle X-ray scattering; SMF, single-molecule fluorescence; smFRET, single-molecule fluorescence resonance energy transfer; Tau, microtubule-associated protein tau; Rama, Ramachandran; RDC, residual dipolar coupling; R_{ee}, end-to-end distance; R_g, radius of gyration; RMSD, root-mean-squared deviation; WT, wild type

REFERENCES

(1) Faísca, P. F. N.; Nunes, A.; Travasso, R. D. M.; Shakhnovich, E. I. Non-Native Interactions Play an Effective Role in Protein Folding Dynamics. *Protein Sci.* **2010**, *19* (11), 2196−2209.

(2) Vendruscolo, M. Proteome Folding and Aggregation. *Curr. Opin Struct Biol.* **2012**, *22* (2), 138−143.

(3) Jahn, T. R.; Radford, S. E. Folding versus Aggregation: Polypeptide Conformations on Competing Pathways. *Arch. Biochem. Biophys.* **2008**, *469* (1), 100−117.

(4) Kulkarni, P.; Bhattacharya, S.; Achuthan, S.; Behal, A.; Jolly, M. K.; Kotnala, S.; Mohanty, A.; Rangarajan, G.; Salgia, R.; Uversky, V. Intrinsically Disordered Proteins: Critical Components of the Wetware. *Chem. Rev.* **2022**, *122* (6), 6614−6633.

(5) Biesaga, M.; Frigolé-Vivas, M.; Salvatella, X. Intrinsically Disordered Proteins and Biomolecular Condensates as Drug Targets. *Curr. Opin Chem. Biol.* **2021**, *62*, 90−100.

(6) Thomasen, F. E.; Lindorff-Larsen, K. Conformational Ensembles of Intrinsically Disordered Proteins and Flexible Multidomain Proteins. *Biochem. Soc. Trans.* **2022**, *50* (1), 541−554.

(7) Fisher, C. K.; Stultz, C. M. Constructing Ensembles for Intrinsically Disordered Proteins. *Curr. Opin Struct Biol.* **2011**, *21* (3), 426−431.

(8) Czaplewski, C.; Gong, Z.; Lubecka, E. A.; Xue, K.; Tang, C.; Liwo, A. Recent Developments in Data-Assisted Modeling of Flexible Proteins. *Frontiers in Molecular Biosciences* **2021**, *8*, DOI: 10.3389/fmolb.2021.765562.

(9) Gong, X.; Zhang, Y.; Chen, J. Advanced Sampling Methods for Multiscale Simulation of Disordered Proteins and Dynamic Interactions. *Biomolecules* **2021**, *11* (10), 1416.

(10) Shea, J.-E.; Best, R. B.; Mittal, J. Physics-Based Computational and Theoretical Approaches to Intrinsically Disordered Proteins. *Curr. Opin. Struct. Biol.* **2021**, *67*, 219−225.

(11) Ramanathan, A.; Ma, H.; Parvatikar, A.; Chennubhotla, S. C. Artificial Intelligence Techniques for Integrative Structural Biology of Intrinsically Disordered Proteins. *Curr. Opin Struct Biol.* **2021**, *66*, 216−224.

(12) Feldman, H.; Hogue, C. A Fast Method to Sample Real Protein Conformational Space. *Proteins: Struct., Funct., Bioinf.* **2000**, *39*, 112−131.

(13) Feldman, H. J.; Hogue, C. W. V. Probabilistic Sampling of Protein Conformations: New Hope for Brute Force? *Proteins* **2002**, *46* (1), 8−23.

(14) Ozenne, V.; Bauer, F.; Salmon, L.; Huang, J.; Jensen, M. R.; Segard, S.; Bernadó, P.; Charavay, C.; Blackledge, M. Flexible-Meccano: A Tool for the Generation of Explicit Ensemble Descriptions of Intrinsically Disordered Proteins and Their Associated Experimental Observables. *Bioinformatics* **2012**, *28* (11), 1463−1470.

(15) Ferrie, J. J.; Petersson, E. J. A Unified De Novo Approach for Predicting the Structures of Ordered and Disordered Proteins. *J. Phys. Chem. B* **2020**, *124* (27), 5538−5548.

(16) Estaña, A.; Sibille, N.; Delaforge, E.; Vaisset, M.; Cortés, J.; Bernadó, P. Realistic Ensemble Models of Intrinsically Disordered Proteins Using a Structure-Encoding Coil Database. *Structure* **2019**, *27* (2), 381−391.

(17) Bank, R. P. D. *RCSB PDB: Homepage.* https://www.rcsb.org/ (accessed 2022-03-26).

(18) Berman, H. M.; Westbrook, J.; Feng, Z.; Gilliland, G.; Bhat, T. N.; Weissig, H.; Shindyalov, I. N.; Bourne, P. E. The Protein Data Bank. *Nucleic Acids Res.* 2000, 28 (1), 235−242.

(19) Pietrek, L. M.; Stelzl, L. S.; Hummer, G. Hierarchical Ensembles of Intrinsically Disordered Proteins at Atomic Resolution in Molecular Dynamics Simulations. *J. Chem. Theory Comput.* 2020, 16 (1), 725−737.

(20) Krzeminski, M.; Marsh, J. A.; Neale, C.; Choy, W.-Y.; Forman-Kay, J. D. Characterization of Disordered Proteins with ENSEMBLE. *Bioinformatics* 2013, 29 (3), 398−399.

(21) Salmon, L.; Nodet, G.; Ozenne, V.; Yin, G.; Jensen, M. R.; Zweckstetter, M.; Blackledge, M. NMR Characterization of Long-Range Order in Intrinsically Disordered Proteins. *J. Am. Chem. Soc.* 2010, 132 (24), 8407−8418.

(22) Lincoff, J.; Haghighatlari, M.; Krzeminski, M.; Teixeira, J. M. C.; Gomes, G.-N. W.; Gradinaru, C. C.; Forman-Kay, J. D.; Head-Gordon, T. Extended Experimental Inferential Structure Determination Method in Determining the Structural Ensembles of Disordered Protein States. *Commun. Chem.* 2020, 3 (1), 74.

(23) Brookes, D. H.; Head-Gordon, T. Experimental Inferential Structure Determination of Ensembles for Intrinsically Disordered Proteins. *J. Am. Chem. Soc.* 2016, 138 (13), 4530−4538.

(24) Bottaro, S.; Bengtsen, T.; Lindorff-Larsen, K. Integrating Molecular Simulation and Experimental Data: A Bayesian/Maximum Entropy Reweighting Approach. *Methods Mol. Biol.* 2020, 2112, 219−240.

(25) Fisher, C. K.; Huang, A.; Stultz, C. M. Modeling Intrinsically Disordered Proteins with Bayesian Statistics. *J. Am. Chem. Soc.* 2010, 132 (42), 14919−14927.

(26) Fisher, C. K.; Ullman, O.; Stultz, C. M. Efficient Construction of Disordered Protein Ensembles in a Bayesian Framework with Optimal Selection of Conformations. *Pac Symp. Biocomput* 2012, 82−93.

(27) Hummer, G.; Köfinger, J. Bayesian Ensemble Refinement by Replica Simulations and Reweighting. *J. Chem. Phys.* 2015, 143 (24), 243150.

(28) Mantsyzov, A. B.; Maltsev, A. S.; Ying, J.; Shen, Y.; Hummer, G.; Bax, A. A Maximum Entropy Approach to the Study of Residue-Specific Backbone Angle Distributions in α-Synuclein, an Intrinsically Disordered Protein. *Protein Sci.* 2014, 23 (9), 1275−1290.

(29) Fawzi, N. L.; Phillips, A. H.; Ruscio, J. Z.; Doucleff, M.; Wemmer, D. E.; Head-Gordon, T. Structure and Dynamics of the Aβ21−30 Peptide from the Interplay of NMR Experiments and Molecular Simulations. *J. Am. Chem. Soc.* 2008, 130 (19), 6145−6158.

(30) Ball, K. A.; Phillips, A. H.; Nerenberg, P. S.; Fawzi, N. L.; Wemmer, D. E.; Head-Gordon, T. Homogeneous and Heterogeneous Tertiary Structure Ensembles of Amyloid-β Peptides. *Biochemistry* 2011, 50 (35), 7612−7628.

(31) Ball, K. A.; Phillips, A. H.; Wemmer, D. E.; Head-Gordon, T. Differences in β-Strand Populations of Monomeric Aβ40 and Aβ42. *Biophys. J.* 2013, 104 (12), 2714−2724.

(32) Ball, K. A.; Wemmer, D. E.; Head-Gordon, T. Comparison of Structure Determination Methods for Intrinsically Disordered Amyloid-β Peptides. *J. Phys. Chem. B* 2014, 118 (24), 6405−6416.

(33) Pitera, J. W.; Chodera, J. D. On the Use of Experimental Observations to Bias Simulated Ensembles. *J. Chem. Theory Comput.* 2012, 8 (10), 3445−3451.

(34) Cesari, A.; Gil-Ley, A.; Bussi, G. Combining Simulations and Solution Experiments as a Paradigm for RNA Force Field Refinement. *J. Chem. Theory Comput.* 2016, 12 (12), 6192−6200.

(35) Bonomi, M.; Camilloni, C.; Cavalli, A.; Vendruscolo, M. Metainference: A Bayesian Inference Method for Heterogeneous Systems. *Science Advances* 2016, 2 (1), e1501177.

(36) Stelzl, L. S.; Pietrek, L. M.; Holla, A.; Oroz, J.; Sikora, M.; Köfinger, J.; Schuler, B.; Zweckstetter, M.; Hummer, G. Global Structure of the Intrinsically Disordered Protein Tau Emerges from Its Local Structure. *JACS Au* 2022, 2, 673.

(37) Li, J.; Zhang, O.; Lee, S.; Namini, A.; Liu, Z. H.; Teixeira, J. M. C.; Forman-Kay, J. D.; Head-Gordon, T. *Learning Correlations between Internal Coordinates to Improve 3D Cartesian Coordinates for Proteins*; arXiv:2205.04676, 2022.

(38) Wang, G.; Dunbrack, R. L., Jr. PISCES: A Protein Sequence Culling Server. *Bioinformatics* 2003, 19 (12), 1589−1591.

(39) Joosten, R. P.; te Beek, T. A. H.; Krieger, E.; Hekkelman, M. L.; Hooft, R. W. W.; Schneider, R.; Sander, C.; Vriend, G. A Series of PDB Related Databases for Everyday Needs. *Nucleic Acids Res.* 2011, 39 (suppl_1), D411−D419.

(40) Kabsch, W.; Sander, C. Dictionary of Protein Secondary Structure: Pattern Recognition of Hydrogen-Bonded and Geometrical Features. *Biopolymers* 1983, 22 (12), 2577−2637.

(41) Ackerman, M. S.; Shortle, D. Robustness of the Long-Range Structure in Denatured Staphylococcal Nuclease to Changes in Amino Acid Sequence. *Biochemistry* 2002, 41 (46), 13791−13797.

(42) Camilloni, C.; De Simone, A.; Vranken, W. F.; Vendruscolo, M. Determination of Secondary Structure Populations in Disordered States of Proteins Using Nuclear Magnetic Resonance Chemical Shifts. *Biochemistry* 2012, 51 (11), 2224−2231.

(43) Nielsen, J. T.; Mulder, F. A. A. CheSPI: Chemical Shift Secondary Structure Population Inference. *J. Biomol NMR* 2021, 75 (6−7), 273−291.

(44) Bhowmick, A.; Head-Gordon, T. A Monte Carlo Method for Generating Side Chain Structural Ensembles. *Structure* 2015, 23 (1), 44−55.

(45) Trivedi, R.; Nagarajaram, H. A. Amino Acid Substitution Scoring Matrices Specific to Intrinsically Disordered Regions in Proteins. *Sci. Rep* 2019, 9 (1), 16380.

(46) MacArthur, M. W.; Thornton, J. M. Influence of Proline Residues on Protein Conformation. *J. Mol. Biol.* 1991, 218 (2), 397−412.

(47) Ting, D.; Wang, G.; Shapovalov, M.; Mitra, R.; Jordan, M. I.; Dunbrack, R. L. Neighbor-Dependent Ramachandran Probability Distributions of Amino Acids Developed from a Hierarchical Dirichlet Process Model. *PLoS Comput. Biol.* 2010, 6 (4), e1000763.

(48) Shen, Y.; Roche, J.; Grishaev, A.; Bax, A. Prediction of Nearest Neighbor Effects on Backbone Torsion Angles and NMR Scalar Coupling Constants in Disordered Proteins. *Protein Sci.* 2018, 27 (1), 146−158.

(49) van Beusekom, B.; Joosten, K.; Hekkelman, M. L.; Joosten, R. P.; Perrakis, A. Homology-Based Loop Modeling Yields More Complete Crystallographic Protein Structures. *IUCrJ.* 2018, 5 (5), 585−594.

(50) Naullage, P. M.; Haghighatlari, M.; Namini, A.; Teixeira, J. M. C.; Li, J.; Zhang, O.; Gradinaru, C. C.; Forman-Kay, J. D.; Head-Gordon, T. Protein Dynamics to Define and Refine Disordered Protein Ensembles. *J. Phys. Chem. B* 2022, 126 (9), 1885−1894.

(51) Nash, P.; Tang, X.; Orlicky, S.; Chen, Q.; Gertler, F. B.; Mendenhall, M. D.; Sicheri, F.; Pawson, T.; Tyers, M. Multisite Phosphorylation of a CDK Inhibitor Sets a Threshold for the Onset of DNA Replication. *Nature* 2001, 414 (6863), 514−521.

(52) Bridi, J. C.; Hirth, F. Mechanisms of α-Synuclein Induced Synaptopathy in Parkinson's Disease. *Front. Neurosci.* 2018, 12, DOI: 10.3389/fnins.2018.00080.

(53) Hurley, T. D.; Yang, J.; Zhang, L.; Goodwin, K. D.; Zou, Q.; Cortese, M.; Dunker, A. K.; DePaoli-Roach, A. A. Structural Basis for Regulation of Protein Phosphatase 1 by Inhibitor-2. *J. Biol. Chem.* 2007, 282 (39), 28874−28883.

(54) Higuchi, M.; Lee, V. M.-Y.; Trojanowski, J. Q. Tau and Axonopathy in Neurodegenerative Disorders. *Neuromol Med.* 2002, 2 (2), 131−150.

(55) Raabe, T.; Olivier, J. P.; Dickson, B.; Liu, X.; Gish, G. D.; Pawson, T.; Hafen, E. Biochemical and Genetic Analysis of the Drk SH2/SH3 Adaptor Protein of Drosophila. *EMBO J.* 1995, 14 (11), 2509−2518.

(56) Mittag, T.; Orlicky, S.; Choy, W.-Y.; Tang, X.; Lin, H.; Sicheri, F.; Kay, L. E.; Tyers, M.; Forman-Kay, J. D. Dynamic Equilibrium

Engagement of a Polyvalent Ligand with a Single-Site Receptor. *Proc. Natl. Acad. Sci. U. S. A.* **2008**, *105* (46), 17772−17777.

(57) Mittag, T.; Marsh, J.; Grishaev, A.; Orlicky, S.; Lin, H.; Sicheri, F.; Tyers, M.; Forman-Kay, J. D. Structure/Function Implications in a Dynamic Complex of the Intrinsically Disordered Sic1 with the Cdc4 Subunit of an SCF Ubiquitin Ligase. *Structure* **2010**, *18* (4), 494−506.

(58) Liu, B.; Chia, D.; Csizmok, V.; Farber, P.; Forman-Kay, J. D.; Gradinaru, C. C. The Effect of Intrachain Electrostatic Repulsion on Conformational Disorder and Dynamics of the Sic1 Protein. *J. Phys. Chem. B* **2014**, *118* (15), 4088−4097.

(59) Das, T.; Eliezer, D. Probing Structural Changes in Alpha-Synuclein by Nuclear Magnetic Resonance Spectroscopy. *Methods Mol. Biol.* **2019**, *1948*, 157−181.

(60) Ahmed, M. C.; Skaanning, L. K.; Jussupow, A.; Newcombe, E. A.; Kragelund, B. B.; Camilloni, C.; Langkilde, A. E.; Lindorff-Larsen, K. Refinement of α-Synuclein Ensembles Against SAXS Data: Comparison of Force Fields and Methods. *Front. Mol. Biosci.* **2021**, *8*, DOI: 10.3389/fmolb.2021.654333.

(61) Auluck, P. K.; Caraveo, G.; Lindquist, S. α-Synuclein: Membrane Interactions and Toxicity in Parkinson's Disease. *Annu. Rev. Cell Dev Biol.* **2010**, *26*, 211−233.

(62) Dedmon, M. M.; Lindorff-Larsen, K.; Christodoulou, J.; Vendruscolo, M.; Dobson, C. M. Mapping Long-Range Interactions in α-Synuclein Using Spin-Label NMR and Ensemble Molecular Dynamics Simulations. *J. Am. Chem. Soc.* **2005**, *127* (2), 476−477.

(63) Bertoncini, C. W.; Jung, Y.-S.; Fernandez, C. O.; Hoyer, W.; Griesinger, C.; Jovin, T. M.; Zweckstetter, M. Release of Long-Range Tertiary Interactions Potentiates Aggregation of Natively Unstructured Alpha-Synuclein. *Proc. Natl. Acad. Sci. U. S. A.* **2005**, *102* (5), 1430−1435.

(64) Sung, Y.; Eliezer, D. Residual Structure, Backbone Dynamics, and Interactions within the Synuclein Family. *J. Mol. Biol.* **2007**, *372* (3), 689−707.

(65) Dancheck, B.; Nairn, A. C.; Peti, W. Detailed Structural Characterization of Unbound Protein Phosphatase 1 Inhibitors. *Biochemistry* **2008**, *47* (47), 12346−12356.

(66) Marsh, J. A.; Dancheck, B.; Ragusa, M. J.; Allaire, M.; Forman-Kay, J. D.; Peti, W. Structural Diversity in Free and Bound States of Intrinsically Disordered Protein Phosphatase 1 Regulators. *Structure* **2010**, *18* (9), 1094−1103.

(67) Zeng, Y.; Yang, J.; Zhang, B.; Gao, M.; Su, Z.; Huang, Y. The Structure and Phase of Tau: From Monomer to Amyloid Filament. *Cell. Mol. Life Sci.* **2021**, *78* (5), 1873−1886.

(68) Bibow, S.; Ozenne, V.; Biernat, J.; Blackledge, M.; Mandelkow, E.; Zweckstetter, M. Structural Impact of Proline-Directed Pseudo-phosphorylation at AT8, AT100, and PHF1 Epitopes on 441-Residue Tau. *J. Am. Chem. Soc.* **2011**, *133* (40), 15842−15845.

(69) Melková, K.; Zapletal, V.; Narasimhan, S.; Jansen, S.; Hritz, J.; Škrabana, R.; Zweckstetter, M.; Ringkjøbing Jensen, M.; Blackledge, M.; Žídek, L. Structure and Functions of Microtubule Associated Proteins Tau and MAP2c: Similarities and Differences. *Biomolecules* **2019**, *9* (3), 105.

(70) Mazouchi, A.; Zhang, Z.; Bahram, A.; Gomes, G.-N.; Lin, H.; Song, J.; Chan, H. S.; Forman-Kay, J. D.; Gradinaru, C. C. Conformations of a Metastable SH3 Domain Characterized by SmFRET and an Excluded-Volume Polymer Model. *Biophys. J.* **2016**, *110* (7), 1510−1522.

(71) Borcherds, W.; Bremer, A.; Borgia, M. B.; Mittag, T. How Do Intrinsically Disordered Protein Regions Encode a Driving Force for Liquid-Liquid Phase Separation? *Curr. Opin Struct Biol.* **2021**, *67*, 41−50.

(72) Ruff, K. M.; Pappu, R. V.; Holehouse, A. S. Conformational Preferences and Phase Behavior of Intrinsically Disordered Low Complexity Sequences: Insights from Multiscale Simulations. *Curr. Opin Struct Biol.* **2019**, *56*, 1−10.

(73) Harrison, P. M. Exhaustive Assignment of Compositional Bias Reveals Universally Prevalent Biased Regions: Analysis of Functional Associations in Human and Drosophila. *BMC Bioinformatics* **2006**, *7* (1), 441.

(74) Wootton, J. C. Non-Globular Domains in Protein Sequences: Automated Segmentation Using Complexity Measures. *Computers & Chemistry* **1994**, *18* (3), 269−285.

(75) Marsh, J. A.; Forman-Kay, J. D. Ensemble Modeling of Protein Disordered States: Experimental Restraint Contributions and Validation. *Proteins* **2012**, *80* (2), 556−572.

(76) Pettersen, E. F.; Goddard, T. D.; Huang, C. C.; Couch, G. S.; Greenblatt, D. M.; Meng, E. C.; Ferrin, T. E. UCSF Chimera—A Visualization System for Exploratory Research and Analysis. *J. Comput. Chem.* **2004**, *25* (13), 1605−1612.

(77) Alderson, T. R.; Pritišanac, I.; Moses, A. M.; Forman-Kay, J. D. Systematic Identification of Conditionally Folded Intrinsically Disordered Regions by AlphaFold2. 2022, DOI: 10.1101/2022.02.18.481080.

(78) Robustelli, P.; Piana, S.; Shaw, D. E. Developing a Molecular Dynamics Force Field for Both Folded and Disordered Protein States. *Proc. Natl. Acad. Sci. U. S. A.* **2018**, *115* (21), E4758−E4766.

(79) Bhattacharya, S.; Lin, X. Recent Advances in Computational Protocols Addressing Intrinsically Disordered Proteins. *Biomolecules* **2019**, *9* (4), 146.